Authors: We would like to thank the anonymous referee for his/her interest and the comments on our manuscript. Bellow we provide a point by point answer to the issues raised by referee #1

Ref.1: It is indicated in the article that "ICAR model was used to obtain a finer 1 km x 1km spatial grid atmospheric simulation nested in the aforementioned WRF simulation domain.", and the comparisons and error analysis are done for ICAR and ERA5 for temperature and precipitation (Figure 2 and 3), showing that ICAR better performs compared to ERA5, which is rather expected concerning the scaling and processes. It would also be important to see the performance of WRF in comparison with ICAR so that one can be sure that ICAR is superior to WRF and it is worth to do such a downscaling process even though it is rather preferable compared to fine scale WRF simulation. This is also valid for the comments on reproduction of snowpack by ICARand ERA5.

Authors: It is mostly true that there is an expected improvement of the ICAR simulation compared with ERA5 as consequence of its higher resolution. This is obvious concerning the temperature because of the smoothing of the topography caused by the coarser resolution of ERA5 while it is necessary to remark that there is an added value of using ICAR for simulating the precipitation which is a much more uncertain variable. The main objective of ICAR was to provide the forcing for the data assimilation scheme that is described later. An intercomparison between ICAR, ERA5 and WRF is a valuable exercise that should be carried out, but it falls outside of the scope of the current manuscript. In our study the comparison between ICAR and the automatic weather stations is performed mostly to define the parameters of the prior probability distribution functions used to perturb the members of FSM2 ensemble of simulations, as is underlined in the text:
"This validation provides a range of uncertainty estimates to generate the probability density functions for the perturbations of the ensemble"
An intercomparison of models should be developed over much more well instrumented areas. We do not consider it appropriate o develop an in depth intercomparison herein, as the results could be extremely constricted by the very low availability of data. In the case of snow, ERA5 is not able to even simulate any snowpack for our domain (as highlighted in the text) as a consequence of the coarse resolution. WRF simulation is able to simulate a very marginal snowpack, as mount Lebanon is too small to reproduce the snowpack at 10 km spatial resolution. Thus, the comparison between models will not show similar results, but this does not mean that each model is not working as expected.

Ref.1: It is better to include topographical and climatological characteristics of AWS (e.g. altitude, aspect, annual average values etc) and comment on these since there are differences in comparison results (e.g. the error difference is less (Figure 2) in the second AWS, it could be assigned to the topographic similarity or just the short period of comparison, but the errors are rather high for the same station in precipitation comparison). This would also be helpful for SWE comparisons in Figure 4.

Authors: We have included a new table summarizing the topographical characteristics of the automatic weather stations and the pixel elevation of ICAR.

Ref.1: The comparison in observed and simulated SWE values is very valuable and worth further discussion. The authors give some details on the inconsistency of comparisons in the third AWS for 2011/2012 which indicates that the observed SWE values might have rather higher values. On the other hand, this inconsistency is also valid for independent snow cover comparison in Figure 5 for the same year, which might indicate some other problems for that year. The consistencies are rather high for the first AWS may be due to its higher altitude, however especially for the second AWS, neither ICAR nor ICAR_assim provides a good performance, for the third AWS, there are varying comparison results and the scale of SWE

(due to extreme value in 2011/2012)makes the graphic rather difficult to interpret. Questions arise on the differences in ICAR and ICAR_assim; assimilation process changes ICAR results dramatically in some years (the second AWS, both years but especially 2015/2016; the third AWS,2010/2011, 2013/2014) while not much for the other years. In some years, assimilation yields significant amount of SWE from almost no snow condition (e.g, the third AWS,first year). On the other hand, assimilation shows very well performance on the first AWS for 2014/2015. Would it be possible to give some explanations on such a big andvarying impact of assimilation?

Authors: There is a very big difference of scale between the ICAR/ICAR_assim simulations and the point-scale AWS observations. Much of the inconsistencies could be explained by this scale mismatch, as the snowpack varies at much finer resolutions at the local scale of the AWS's as explained in paragraph 4.2 Fractional snow cover assimilation.
We hypothesize that The 2011/2012 inconsistency between ICAR_assim and MODIS gap-filled snow cover extent could be explained by the fact that MODIS gapfilled products will be biased during the snow seasons with persistent cloud covers (as the 2011/2012 season), as the gapfilling algorithm will have just a few observations. Thus, the ICAR_assim snow cover exhibits higher values than MODIS as consequence of the low elevation snowpacks. While MODIS gapfilled products will not be able to detect properly such low elevation and very variable snow covers as a consequence of the cloud cover, the particle batch smoother is able to propagate the few fSCA observations through the whole season. However, it is very surprising that the independent observations of Koeniger et al., 2017 highlight the extraordinary snowpack accumulations of the 2011/2012 snow season (as can be observed in the ICAR_assim reanalyses), while it is not observed in the MODIS gapfilled products. To improve the discussion about this topic, we have added the following sentences to the manuscript.
"In addition, the MODIS snow cover products should be considered less accurate over areas of fast melting (Gascoin et al., 2015). Such effect combined with the fact that 2011/2012 snow season showed persistent cloud covers related with its exceptional snowpack, could explain the biases in the Figure 5 2011/2012 snow season, as the gapfilling algorithm had less information to fill the MODIS snow cover time series, while the PBS had propagated the fSCA information through the whole season from the few available observations."
The inconsistencies observed between the AWS and ICAR_assim, are similar to those found in Fayad and Gascoin (2020) using the MICROMET + SNOWMODEL framework. They found that it was not trivial to simulate the snowpack at the AWS locations, even using meteorological observational data from the AWS itself. They hypothesize that the inconsistencies could be related to the partitioning of the precipitation phase, because of the relatively warm conditions close to the 0ºC. In addition, some local effects are probably affecting the AWS data, but unfortunately there is not enough information to study such effects and the inconsistencies should be considered as part of the total uncertainty. Actually, the ICAR_assim and AWS SWE comparison (as for any other grided numerical model) should be taken with care, as the ICAR_assim represents an averaged region (i.e. model grid cell). Thus, the good results showed on the first AWS for 2014/2015 snow season could be completely different if the AWS were at a different location just few meters way, as reported by a manual inspection by Fayad and Gascoin (2020) at 15 of January 2016, cited in the manuscript as follows
"For example, Fayad and Gascoin (2020), reported large differences with the AWS data from insitu measurements on 15 of January 2016, when they measured snow depths up to 258 cm on the surroundings of the third AWS location (Figure 4; bottom panel), while the AWS sensor itself detected 7.5 cm."

Ref1: Concerning a rather constant (or slightly decreasing) relative area in Figure 9 and rather constant SWE values above 2500 m a.s.l. in Figure 8, it is surprising to see an increase in total water storage at 2800 m a.s.l. so it would be nice to give attention to this part.

Authors: Such an increment is caused by the accumulated surface over 2800 masl, combined with the very high values of SWE at the higher elevations. Actually, in the figures 9 and 10 the relative area above 2800 masl is slightly higher than the previous elevations. We have modified the figures 9 and 10 to include the label >2800 to clarify this.

Specific comments:

Ref1: Since ICAR_assim is already produced by assimilating MODIS through ICAR, the comparison in Figure 5 might include ICAR directly instead of ICAR_assim and/or more statistical results can be given on both.

Authors: Figure 5 was designed to show the performance of the PBS, that is why we consider it is better to show ICAR_assim snow cover extent compared with the MODIS gapfilled snow cover extent. To highlight the improvement of the performance after the PBS implementation we have added the statistics of ICAR compared to MODIS gapfilled products.

Ref1: ***In section 4.3, the time period (2010-2017?) should be indicated instead of "recent years" for the explanation of Figure 7.***

Authors: Change accepted, thanks.

Ref1: In paragraph with code "515" there is a repetition for two sentences which should be avoided.

Authors: Corrected, thanks

Authors: We would like to thank the anonymous referee for his/her interest and the comments on our manuscript. Bellow we provide a point by point answer to the issues raised by referee #2

Ref.2: Line 45: Could the authors be more precise with deep and long lasting snowpacks? How deep and how long? Are those common characteristics of snowpack in all Mediterranean mountains?

Authors: There is not an obvious answer to these questions. The depth and duration of the snowpack are often related to the elevation. As is stated in the text, the Mediterranean snowpacks are deep and persistent, as long as the range has a sufficient elevation, due to the wintertime distribution of the precipitation of Mediterranean climates. The references supporting such a statement (Alonso-González et al., 2020; Fayad et al., 2017b) are much more extensive with several data at different locations and elevations. We have added to the following to the text:
"...snowpacks accumulating more than 3 meters and lasting more than 5 months at the summit areas"

Ref.2: Line 47 and 48 and Line 51: Does the interannual variability referred in Line 51 any influence in the reshape of the hydrographs? I might think yes.

Authors: Yes it does. We have modified the text as follows:
"Mediterranean snowpacks are characterized by a high interannual variability, which affect the amount and seasonality of river flows"

Ref.2: Lines 100-102: There are many works in combining numerical modelling and remote sensing using data assimilation techniques. Please try to be less categorical in your statement.

Authors: We have removed the following sentence:
"However, less often, numerical modeling and remote sensing have been combined in a data assimilation framework to study the multiyear snowpack dynamics."

Ref.2: Lines 107-126: I miss the aim of the research in this paragraph, what is relevant scientific question addressed by this work? The paragraph seems more a summary of a methodological section.

Authors: We have added the following sentence to the text:
"The objectives here are: i) to explore the potential of a methodology to develop a snowpack reanalysis over data scarce regions and ii) to describe the main snowpack dynamics over the Lebanese mountains being the first use of ICAR for this approach"

Ref.2: Line 129: Could the authors provide some data or references about this typical Mediter-ranean climatology?

Authors: We have added the following reference to the text:
Peel, M. C., Finlayson, B. L., and McMahon, T. A.: Updated world map of the Köppen-Geiger climate classification, Hydrol. Earth Syst. Sci., 11, 1633–1644, https://doi.org/10.5194/hess-11-1633-2007, 2007.

Ref.2: Line 139: The authors mentioned here that the mountainous ranges act as a barrier to humidity advected from the sea. Could you provide some data about physiographic (elevation, slopes, land covers) and meteorological characteristics that differentiate both mountainous ranges?

Authors: We consider that Fig1 describes elevations and slopes and the Jomaa et al. (2019) support such a statement about the orographic precipitation. We have added the following sentence referring to the land cover:
“Lebanese mountains are highly karstified encouraging the infiltration of rainfall and snowmelt. The land cover is mostly composed of bare rocks and soils with irregularly distributed patches of shrubland, oak and pine forest.”

Ref.2: Line 158: Could the authors clarify what are they referring with previously?

Authors: We have change “Previously” by “First”.

Ref.2: Line 162: Why do the authors chose 35 levels and 50hPa?

Authors: This is the regular WRF configuration. As there is limited information in our domain, we had to choose a regular model set up. We have added the following sentence to the text:
“similarly to other studies over Mediterranean climate (Arasa et al (2016))”
Arasa, R. , Porras, I. , Domingo-Dalmau, A. , Picanyol, M. , Codina, B. , González, M. and Piñón, J. (2016) Defining a Standard Methodology to Obtain Optimum WRF Configuration for Operational Forecast: Application over the Port of Huelva (Southern Spain). Atmospheric and Climate Sciences, 6, 329-350. doi: 10.4236/acs.2016.62028.

Ref.2: Line 166: Which version of WRF is been used?

Authors: We have added “3.8 version” to the text.

Ref.2: Line 172-180: The authors justify the use of a specific parameterization schemes in the WRF simulation base on Ikeda et al., (2010) a study performed over Colorado. I can understand similitudes regarding topography of both areas. However, the sizes of both mountainous ranges, the proximity to the sea are different. What are the influences of having choose the same parameterization? Since the lack of data does not allow a deeper analysis, could you explain a bit deeper the physical reasons behind the selection of this atmospheric parameterization?

Authors: As referee.3 highlights there is not a way to test different WRF parameterizations here. Thus, there is a need for assumptions. However, the reason for using an atmospheric model as forcing is actually the lack of observational data allowing to work over areas and times where it is not possible to find any information. There is probably not any physical reason to choose a specific WRF set up. Most of the studies looking for perfect WRF configurations are factorial experiments over well monitored/instrumented areas, as it is not easy to offer physically based explanations about why a particular parameterization performs better than others.
Despite thefact that all the parameterizations used in the WRF simulation (as well as its alternatives) are physically based, there are many empirical components inside them that are impossible to avoid. Thus, we can not justify choosing a parameterezation over the region different from what the literature recommends, as all the parameterizations concern physics and at some point over empirical approximations. This is where the importance of the data assimilation becomes crucial, correcting the uncertainty caused by parameterizations and observations, exploiting the strengths and weaknesses of both.

Ref.2: Line 204: Do the authors mean they are not considering any convective process in their simulation? What are the implications?

Authors: Convection can not be represented by the linear theory simplification and therefore by ICAR. The convective schemes of ICAR are highly experimental and in most cases becomes the model unstable making it crash at 1km resolution. The implications for winter precipitation are probably related to the amount of precipitation, but are much less significant than during the summer season. Such effects should be compensated by the PBS if it has some impact on the snowpack. We have added the following clarification to the text:

"The lack of convection could have some impact on the total amount of precipitation, and therefore on the seasonal snowpack. However, such deviations in the total amount of precipitation are compensated by the PBS."

Ref.2: Line 220: What is the temporal resolution of Theia? And therefore, how many days of overlapping between Theia and MODIS do you have? Is this overlapping constant during the year? Could that introduce errors in the transformation function?

Authors: The revisit period of Sentinel-2 is at least 5 days since the launch of Sentinel-2B (i.e. after march 2017). It can be even less in areas where successive swaths overlap laterally (every 2 and 3 days). As written in the manuscript we have used a total of 645 Sentinel-2 snow images. This corresponds to all available images from 03 Sep 2017 to 24 Dec 2018 over Lebanon (five Sentinel-2 tiles: T36SYB, T36SYC, T36SYD, T37SBT, T37SBU). For every Sentinel-2 image we can match a MODIS image since there is a MODIS image every day over Lebanon during the same period. However, the number of Sentinel-2/MODIS images is a bit misleading since large parts of a single image can be covered by cloud, or correspond to the sea surface. In addition we only extracted Sentinel-2 pixels where MODIS NDSI is strictly positive (i.e. MODIS snow covered pixels) to establish the relationship between MODIS NDSI and Sentinel-2 fSCA. Therefore we think it is more informative to provide the number of pixels that were actually used to optimize the fSCA function (5.84e4). We will clarify this in the text accordingly.

Ref.2: Line 226-228: How do the authors choose this 40% of the data? Why do the authors use a bigger number of data for calibration than for validation? Could the authors show the same errors in the calibration phase to see differences? I think the reader would be interested in see the fitting graph

Authors: In fact we used 40% for calibration (L226), therefore we used a bigger number of data for validation. By using a larger fraction of data for validation we expect to have a more robust estimate of the model accuracy. We will include the graph of the model calibration in supplement of the revised manuscript.

Ref.2: Line 234: The authors mentioned here the difference between revisiting times of Aqua and Sentinel-2, but what is the Terra revisiting time in the area?

Thank you for this comment, it is approximately 10:30 A.M. local time dailly, i.e. similar to Sentinel-2. We will add this information in the revised manuscript.

Ref.2: Line 240: When the authors say "empty" are they referring to a non-snow cell or a non-information cell? Why have the authors chosen that option instead of an interpolation with nearest cells?

Authors: We consider it a non-information cell (changed in the text for clarification). The reason for this is to not propagate into the reanalysis information derived from interpolations. As a smoother, the PBS can propagate the information over the whole season (forward and backward in time), with this information being the trajectory of the fSCA the variable that is assimilated. There is not any

added value on including a few more noise cells derived from incomplete observations, especially in a Mediterranean area like Lebanon where persistent cloud cover is not expected.

Ref.2: Line 259: How do the authors apply the FSM2 snow model in a distributed way? In the last paragraph of this section it seems the authors use some depletion curve for that. However, it is not clear if that is just part of the assimilation or plays a role in the actual snow modelling. Could the authors add a sentence in this paragraph specifying how that is done?

Authors: There is not any specific FSM set-up to implement it in a distributed way. What we did was implement the PBS grid cell by grid cell, generating the distributed reanalysis. The subgrid depletion curve was used to translate the grid cell scale FSM outputs to fSCA (within each cell) to make it possible to assimilate the MODIS information. This is the regular way to assimilate fSCA into snow models: independently for each grid cell and snow season. The methodology is explained in Line 290, see also Line 300:
"The PBS was implemented over the fSCA ensemble over each grid cell and season independently"

Ref.2: Line 270: Why do the authors chose a log-normal and a normal gaussian probability density function? Are just precipitation and temperature the inputs/forcing variables ofthe FSM2 snow model? If they are more than precipitation and temperature, how are you perturbing them in the assimilation scheme?

Authors: We use a lognormally distributed multiplicative parameter to perturb the precipitation and a normally (Gaussian) distributed additive parameter to perturb the air temperature. A lognormal distribution, which only has positive support, is chosen for the multiplicative precipitation perturbation parameter since precipitation can't be negative, while a normal distribution, which has both negative and positive support, is chosen for the additive temperature perturbation parameter to allow for both positive and negative additive perturbations. So, aligned with the Bayesian underpinnings of data assimilation (Wikle and Berliner, 2007), we are selecting the distributions for these uncertain parameters based on physical constraints and prior knowledge. Note that these forcing perturbations are closely in line with previous applications of the PBS for snow reanalysis (e.g. Margulis et al., 2015; Cortes et al., 2015; Fiddes et al., 2019). The energy and mass balances in FSM are driven by standard hydrometeorological forcing variables; i.e. near surface air temperature, wind speed, specific humidity, precipitation, and incoming longwave and shortwave radiation. The reason that we do not perturb more forcing parameters is that by doing so we would enlarge the dimensions of the parameter space which, due to the curse of dimensionality, would make degeneracy more likely with the PBS especially since we are assimilating a relatively large number of independent observations (van Leeuwen 2009; Margulis et al., 2015). Our choice of perturbing precipitation (whose phase is controlled by air temperature) in particular is justified by the fact that precipitation bias is often the key uncertain factor controlling physically-based snow models (Raleigh et al., 2015).

New references:
Wikle and Berliner (2007), A Bayesian Tutorial for Data Assimilation, Physica D, https://doi.org/10.1016/j.physd.2006.09.017
Raleigh et al. (2015), Exploring the impact of forcing error characteristics on physically based snow simulations within a global sensitivity analysis framework, HESS, https://doi.org/10.5194/hess-19-3153-2015

Ref.2: Line 319: How was the snow depth measured? Why not to do the comparison in term of snow depths avoiding to use a constant density value? Reading Essery (2015)FMS2 provides snow depth as an output.

Authors: As explained in the text, we wanted to compare the snow output of the ICAR model directly, which is provided just in terms of SWE.

Ref.2: Lines 328-342: The methodology explained here is not clear. Neither the reasoning behind nor the way SWE is compared against satellite observation. Are you using SWE measuring using remote sensing?

Authors: We have split the paragraph in two different ones at line 330. It helps to clarify this as the SWE comparison is not related with the remote sensing part.

Ref.2: Lines 345-381: I miss numbers supporting the statements throughout the section. Here a few examples: "Figure 2 shows how the ICAR model was able to improve the 2 m air temperature data, compared with ERA5 reanalysis", "ICAR reduces the spread of the daily precipitation errors". Moreover, I think it could be interesting to analyse a deeper when the error between observations and simulations occurs. Are they bigger in winter than in summer? Is there any dependence with the total precipitation of the hydrological year (dry or wet)? It may have large impact in your results.

Authors: We have added numbers to the statements of the section. We agree that a deeper error assessment of ICAR should be done as it is a very new regional atmospheric model under continuous development. However, the mountains of Lebanon are not an appropriate location to do this in due to the limited data availability. As for the suggestions: i) here there is no observed information in summer (Fig. 2 and 3) and ii) it is not possible to define the dry and wet years due to the very short length of the observed series (Fig.3).

Ref.2: Figure 3: In general, ICAR precipitation values seems to be higher than ERA5 precipitation values. However, the bias in ERA5 are positive and bigger than ICAR. How dothe authors explain that?

Authors: Exactly, the ICAR precipitation values are higher than ERA5 values, but the difference between ERA5 and the observations is bigger than between ICAR and observations. ERA5 is too dry over the area, likely due to the lack of orographical precipitation as consequence of the smooth of the topography of the ERA5 spatial resolution.

Ref.2: Figure 4: How do the authors explain the heterogeneous differences in the assimilation results between years? The authors gave some explanation about one of the years in Lines 399-410, however, could you give deeper explanations about the differences between years in the whole period?

Authors: Fig.4 as well as Fig3 and 2 should be used with caution as highlighted in the text. There is a big scale missmatch between the point scale AWS information and the reanalysis. The reanalysis seems to perform better at higher elevations (Fig4 A and C), suggesting difficulties to model the precipitation partition phase, as other authors have shown over the region (Line 280). It is not possible to offer any convincing reason about the (mostly small) differences in the performance between years. The snow wind redistribution processes strongly controls the snowdepth at the point scale resolution of the AWS making comparisons complicated. In addition, previous studies have highlighted the very high snow depth spatial variability over the area as remarked in the text.

Ref.2: Lines 421-448 and Figure 5: If I read well, here you are comparing the results of your assimilation (ICAR_assim) with the assimilated variable (Obs). This is a prove that your assimilation scheme works well, and therefore, the obtained metrics should be interpreted as

that. The real impact of the assimilation scheme on snow dynamics is the show in the comparison with the independent variable SWE, not assimilated during the process.

Authors: Exactly, to clarify this point we have added the following to the text:
"...showing the potential of fSCA assimilation through the PBS in improving the ICAR SWE products."

Ref.2: Section 4.3: All section is written as if the simulated values were a "ground truth", I would indicate some of the limitations of the performed simulations and all the sources of uncertainty and errors that are conditioning these statements.

Authors: ICAR limitations are already described in lines 349-355. In addition, we have added the following sentences to the section 4.3 :
"ICAR_assim exhibits some limitations that should be considered. First, despite the high resolution of the reanalysis the regional nature of the simulations prevent the representation of some processes like wind or avalanche snow redistribution. In addition, there are some other sources of uncertainty involved in the development of the reanalysis, like the depletion curve, the fSCA derived from MODIS or the structural uncertainty associated with each model. However, ICAR_assim has been shown to be consistent with the few observations providing a valuable resource in the data scarce context of the Lebanese mountains.

Ref.2: Figures 9 and 10: What does the relative area referring to (snow area over the area of the band or area of the band over all area of the mountainous ranges)? It would be interesting to see these two graphs in both mountainous ranges.

Authors: It is already described in the text (Line 501):
"The relative area lying at each elevation compared with the total elevation over 1300 m a.s.l..."
We have added the Lebanon and Anti-Lebanon ranges SWE and accumulated water partition.

Lines 504-508: Could you elaborate more the reasoning in this paragraph?

Authors: We have added the following:
"This suggest that the mean peak SWE series at lower elevations could hide a large variation in mass due to the wider areas at lower elevations *where many different peak SWE values can coexist,...*"

Ref.2: Figure 10: How do you explain that the total storage at 2800 m a.s.l. increases?

Authors: This is because the storage at 2800m a.s.l. integrates all the surface over 2800. We have modified Fig,10 to clarify it.

Technical comments

Ref.2: Figure 1. What are A and B, could the authors specify it in the body text lines 58-62 and in the figure caption.

Authors: Fig1 legend indicates the meaning of A (WRF domain) and B (ICAR domain). We think that in this way it remains clear to readers.
The topic of Lines 58-62 do not match the atmospheric models domains.

Ref.2: A figure with a scheme of the implementation process would help to better understand the complexity of the flow chart followed.

Authors: We have added a schematic flowchart to the Section 3.2.2 summarizing the whole process.

Ref.2: Figures 2, 3 and 4: It is difficult to know in which season of the year you are with the format "Days since". I propose to add actual dates in x-axis of these figures. Moreover, it is complicate to see differences between the 3 represented variables, especially in the precipitation graph. Finally, it is difficult to see what the values of the boxplot are represented, I would recommend here to change the y-axis limits, add, y-axis values and/or a grid.

Authors: We have added the suggested changes.

Authors: We would like to thank the anonymous referee for his/her interest and the comments on our manuscript. Bellow we provide a point by point answer to the issues raised by referee #3.

Ref.3: The paper presents an approach to downscale ERA5 reanalysis by using MODIS fSCA information. Even though the approach is not completely innovative, the research has a high relevance for the application in arid areas. Below detailed comments.

Ref.3: p.3 line 107:please provide here a clear statement about the objectives of the work and the innova-tive part with respect to the current literature.

Authors: We have added the following sentence to the text:
"The objectives here are: i) to explore the potential of a methodology to develop a snowpack reanalysis over data scarce regions and ii) to describe the main snowpack dynamics over the Lebanese mountains being the first use of ICAR for this approach"

Ref.3: Section 3.2.1. More detailed information about the processing of MODIS data need to be introduced here. Please add the new adapted linear function that the authors found by using Theia data and the explanation why it differs from the Salomonson&Appel2004.

Authors: The equation of the linear fit is fSCA [%] = 1.23 x NDSI + 23.48. It differs from the equation of Salomonson and Appel (2004) because the calibration site is different. Salomonson and Appel (2004) obtained their relationship using Landsat-derived fSCA over Alaska, Labrador, and Siberia.

Ref.3: How were MOD and MYD images merged? is there a cloud gap filling procedure? If the use of MYD produces a higher error why do not use only MOD?

Authors: In fact this is what we did (see line 230).

Ref.3: Was a validation with ground measurements conducted? this can provide an independent source of information to better quantify the accuracy of the new proposed linear relationship.

Authors: The scarce snow depth data are already used in the other section of the manuscript. Theia Sentinel-2 snow products were extensively evaluated by Gascoin et al. (2019). For example, the comparison with automatic snow depth measurements in the Alps and Pyrenees showed that the accuracy (proportion of correct classifications) was 94 % and the kappa coefficient was 0.83.

Ref.3: Moreover in the validation, a comparison of the new linear relationship with the one proposed by Salomonson&Appel2004is advisable to understand the advantage of the new approach.

Authors: With the Salomonson and Appel (2004) equation we find slightly larger mean absolute error (6.2% vs 5.7%) and RMSE (12% vs. 11%) (figure below)

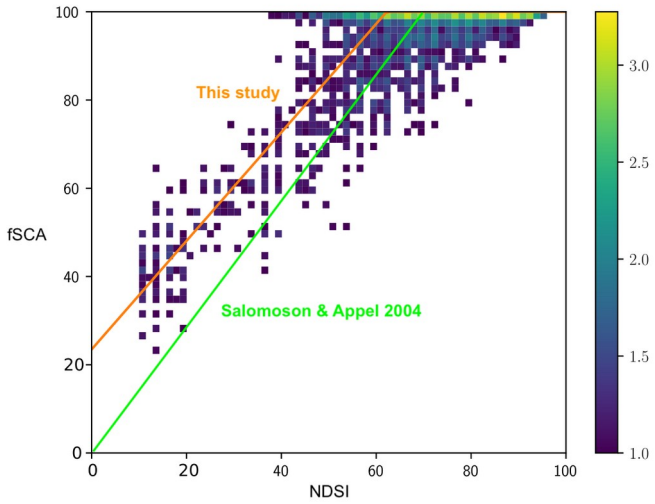

p.9, line 320: as the density can change during the season, please justify the use of the value.

Authors: It is true that density varies during the season. However, we had to use a fixed density value to compare the ICAR snow outputs with the snow depth observations at the AWS. Fayad et al., 2017a showed that such value is the mean density of the snowpack in the area. We showed the uncertainity caused by this value with a sensitivity analysis in Fig. 4

Snowpack dynamics in the Lebanese mountains from quasi-dynamically downscaled ERA5 reanalysis updated by assimilating remotely-sensed fractional snow-covered area

Esteban Alonso-González[1], Ethan Gutmann[2], Kristoffer Aalstad[3], Abbas Fayad[4], Marine Bouchet[5], Simon Gascoin[5]

1- Instituto Pirenaico de Ecología, Spanish Research Council (IPE-CSIC), Zaragoza, Spain
2- Research Application Laboratory, National Center for Atmospheric Research (RAL-NCAR), Boulder, CO, United States
3- Department of Geosciences, University of Oslo, Oslo, Norway
4- Centre for Hydrology, University of Saskatchewan, Saskatoon, Saskatchewan, Canada
5- Centre d'Etudes Spatiales de la Biosphère (CESBIO), UPS/CNRS/IRD/INRA/CNES, Toulouse, France

Abstract: The snowpack over the Mediterranean mountains constitutes a key water resource for the downstream populations. However, its dynamics have not been studied in detail yet in many areas, mostly because of the scarcity of snowpack observations. In this work, we present a characterization of the snowpack over the two mountain ranges of Lebanon. To obtain the necessary snowpack information, we have developed a 1 km regional scale snow reanalysis (ICAR_assim) covering the period 2010-2017. ICAR_assim was developed by means of ensemble-based data assimilation of MODIS fractional snow-covered area (fSCA) through ~~the~~an energy and mass snow balance model the Flexible Snow Model (FSM2), using the Particle Batch Smoother (PBS). The meteorological forcing data was obtained by a regional atmospheric simulation ~~developed through~~from the Intermediate Complexity Atmospheric Research model (ICAR) nested inside a coarser regional simulation ~~developed by~~from the Weather Research and Forecasting model (WRF). The boundary and initial conditions of WRF were provided by the ERA5 atmospheric reanalysis. ICAR_assim showed very good agreement with MODIS gap-filled snow products, with a spatial correlation of R = 0.98 in the snow probability (~~P(snow)~~ $P(snow)$), and a temporal correlation of R = 0.88 in the day of peak snow water equivalent (SWE). Similarly, ICAR_assim has shown a correlation with the seasonal mean SWE of R = 0.75 compared with in-situ observations from Automatic Weather Stations (AWS). The results highlight the high temporal variability of the snowpack in the Lebanon ranges, with differences between Mount Lebanon and Anti-Lebanon that cannot ~~be~~ only be explained by ~~its~~ hypsography ~~been~~with Anti-Lebanon in the rain shadow of Mount Lebanon. The maximum fresh water stored in the snowpack is in the middle elevations approximately between 2200 and 2500 m a.s.l. Thus, the resilience to further warming is low for the snow water resources of Lebanon due to the proximity of the snowpack to the zero isotherm.

Keywords — Snow, dynamical downscaling, data assimilation, fractional snow cover, Mediterranean ~~Mountains~~mountains

1. Introduction

The hydrological processes related to mountain areas are essential for the water supplies to a large part of humanity (Viviroli et al., 2007). Despite the relatively mild temperature of the Mediterranean climates, ~~mountains~~mountains there often exhibits deep and long-lasting ~~snowpacks~~snowpacks accumulating more than 3 meters and an average snow seson of 5 months at the summit areas (Alonso-González et al., 2020; Fayad et al., 2017b). Thus, as most of the annual precipitations falls during winter season (García-Ruiz et al., 2011) the mountain snowpack strongly reshapes the hydrographs to ~~sustaine~~sustain high flows until the end of the spring (López-Moreno and García-Ruiz 2004), permitting better synchronization of water demand and availability during the dry season (García-Ruiz et al., 2011). ~~Mediterranean snowpacks are characterized by a high interannual variability~~Mediterranean snowpacks are characterized by a high interannual variability, which affect the amount and seasonality of river flows. Despite this variability, the thickness and high density exhibited by ~~Mediterranean snowpacks~~the snowpack in the Mediterranean climate (Fayad et al., 2017b), makes them an effective water storage system. In addition, high sublimation rates are associated with Mediterranean snowpacks (Fayad and Gascoin, 2020; Herrero et al., 2016; Schulz and de Jong, 2004). The fact that snowpack conditions are close to isothermal during most of the snow season makes them highly sensitive to the current climate warming (Alonso-González et al., 2020a; López-Moreno et al., 2017; Yilmaz et al., 2019).

The Lebanon ~~Mountains~~mountains are a clear example of Mediterranean ~~mountains~~mountains, where snow exerts a key control on the hydrology and water resources are critically dependent on the interannual fluctuations of the ~~snow pack~~snowpack (El-Fadel et al., 2000). Despite ~~its~~their importance, snow observations in the region are scarce (Fayad et al., 2017a), making the study of distributed snow dynamics challenging. Recently, Fayad and Gascoin (2020) have develop distributed snowpack simulations over key areas of Mount Lebanon, forcing the model by interpolating observations of the few existing ~~a~~Automatic ~~w~~Weather ~~s~~Stations (AWS) using the SnowModel by Liston and Elder (2006). They showed the importance of the liquid water percolation scheme given the isothermal condition of the snowpack and estimated the snow water equivalent over three key catchments in the windward western divide of Mount Lebanon. However, due to the lack of meteorological data outside this area, these simulations did not cover the whole mountain area of the country and were limited to three snow seasons.

Remote sensing and numerical modeling have become reliable tools to generate useful meteorological information for mountain regions (Lundquist et al., 2019), and also to

generate robust snow data worldwide. Atmospheric reanalyses are a valuable source of long term (multidecadal) climatological information, especially at planetary scales (e.g. Wegmann et al., 2017; Wu et al., 2018). However, spatially downscaling such products is mandatory to derive relevant snow information over complex terrain (Baba et al., 2018b; Mernild et al., 2017 among others). Dynamical downscaling has been shown to outperform statistically gridded products for meteorological variables in complex terrain (Gutmann et al., 2012). More specifically, high resolution fully dynamical meteorological models can reproduce the snowfall patterns over complex terrain (Ikeda et al., 2010; Rasmussen et al., 2011). However, the computational cost of fully dynamical downscaling solutions becomes prohibitive for large domains at high spatial resolutions. To reduce the computational cost, many different solutions of varying complexity have been developed using statistical interpolations corrected with the topography or using simplifications of the atmospheric dynamics (Fiddes and Gruber, 2014; Gutmann et al., 2016; Liston and Elder, 2006). In this way, energy and mass balance snowpack models have been coupled with atmospheric models to develop multidecadal snow simulations (Alonso-González et al., 2018; van Pelt et al., 2016 among others). In addition, remote sensing products have been widely used to study the duration and variability of the snow cover (Gascoin et al., 2015; Saavedra et al., 2017; Yilmaz et al., 2019). However, less often, numerical modeling and remote sensing have been combined in a data assimilation framework to study the multiyear snowpack dynamics. Assimilation of remotedremotely sensed snow cover observations has been shown shown considerable potential tofor improveing numerical snowpack models outputs in both distributed (e.g. Baba et al., 2018; Margulis et al., 2016) and semi distributed simulations (Cluzet et al., 2020; Fiddes et al., 2019). These approaches are particularly promising in data-scarce regions to reduce the biases in atmospheric forcing.

In this work, we have simulated the snowpack of the Lebanon Mountainsmountains, as an alternative to sparse snowpack observations. We have generated a 1 km resolution snowpack reanalysis, using an ensemble based assimilation of fractional snow-covered area (fSCA) obtained from the Moderate Resolution Imaging Spectroradiometer (MODIS) satellite sensor. More specifically, the ERA5 reanalysis (Hersbach, 2016) was dynamically downscaled using regional atmospheric models in two steps. First, a 10 km resolution atmospheric simulation using the Weather Research and Forecast model (WRF) (Skamarock et al., 2008) was performed covering the period between 2010 and 2017. Then, a finer 1 km simulation using the Intermediate Complexity Atmospheric Research model (ICAR) (Gutmann et al., 2016) was nested inside the previous WRF simulation covering the same time period. To improve the ICAR snowpack outputs, the new simulated meteorological data generated was used to force an energy and mass balance snowpack model, the Flexible Snow Model (FSM2) (Essery, 2015), previouslywhile perturbing the meteorological fields to generate an ensemble of snowpack simulations. Then, the Particle Batch Smother (PBS) (Margulis et al., 2015), a Bayesian data assimilation scheme, was applied to assimilate daily remotely sensed fSCA information. We tested the generated snow products in the mountainsmountains of

Lebanon with independent observations. Finally, the dynamics of the snowpack in the ~~mountains~~mountains of Lebanon are studied from the generated multi-year snow time series. The objectives of this paper are: i) to explore the potential of a methodology to develop a snowpack reanalysis over data scarce regions and ii) to describe the main snowpack dynamics over the Lebanese mountains. This is the first use of ICAR for generating a snow reanalysis.

2. Study area

Lebanon is a country located on the eastern Mediterranean Sea between latitudes 33° and 35° N. Its climatology ~~is~~ typically Mediterranean (Peel et al., 2007) influenced mainly by its proximity to the Mediterranean Sea and its complex topography (Figure 1). There are two main mountain ranges that run in parallel to the Mediterranean coast from North to South. These mountain ranges are the Mount Lebanon and Anti-Lebanon ~~Mountains~~mountains, reaching 3088 m a.s.l. (Qurnat as Sawdā peak) and 2814 m a.s.l. (Mount Hermon peak) respectively. The Lebanese mountains are highly karstified encouraging the infiltration of rainfall and snowmelt. The land cover is mostly composed of bare rocks and soils with irregularly distributed patches of shrubland, as well as oaks and pine forest.

Despite Lebanon having more available water resources than its neighboring countries, it is considered a water scarce region (El-Fadel et al., 2000), where droughts are frequent and are expected to increase due to climate change (Farajalla et al., 2011). The particular spatial distribution of its mountain ranges constitutes an effective topographical barrier to humidity advected from the Mediterranean sea, enhancing the winter precipitation as a consequence of ~~-~~orographic effects (Jomaa et al., 2019). ~~usTh~~ In these mountain ranges, ~~of the countrywide area a lying over a seasonal snowpack appears every year~~ the combined effects of orography and Mediterranean climate results in yearly seasonal-snowpack over a large part of the country (Mhawej et al., 2014).

It was estimated from satellite retrievals of snow cover that 31% of the spring discharge of Lebanon is associated with snow–melt (Telesca et al., 2014). In addition, the groundwater dynamics of Lebanon are mainly controlled by the snow melt as consequence of its karstic nature (Bakalowicz et al., 2008; El-Fadel et al., 2000). Thus, the water resource provided by the snowpack is crucial for the Lebanese society. ~~The dependence of Lebanon on snow resources became~~ with this need becoming more acute during the recent drought in the Eastern Mediterranean (Cook et al., 2016). In addition, the water stress increased notably in recent years partially due to the increase in domestic water demand, agricultural water use, and the Syrian refugee crisis (Jaafar et al., 2020) but also due to the poor management of the water resources, and water pollution.

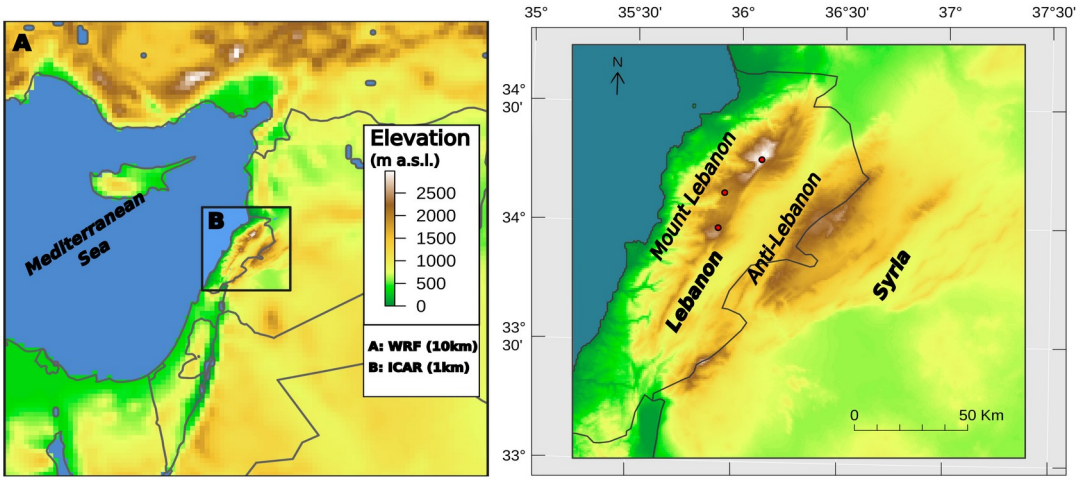

Figure 1: Atmospheric models domain configuration (left) and Lebanon Localization map (right). The red dots represent the AWS positions.

3. Data and Methods

3.1 Regional atmospheric simulations configuration

To generate the meteorological forcing, we used the ICAR atmospheric model nested inside a WRF simulation forced by the ERA5 reanalysis. ~~Previously, t~~The WRF model was used to generate a regional atmospheric simulation on a 10 km x 10 km grid, covering the eastern part of the Mediterranean Sea with 179 x 179 grid cells, centered over Lebanon's ~~Mountains~~mountains (Figure 1). In the vertical dimension, the domain ~~is~~was composed of 35 levels with the top set to 50 hPa, similarly to other studies over Mediterranean regions (Arasa et al., 2016). The simulation covers the period from 01st of January 2010 to 30th of June 2017, using the first 9 months as spin-up period allowing for physical equilibrium between the external for~~gc~~ings and the land model (Montavez et al., 2017). We used the ERA5 reanalysis dataset at an hourly frequency as boundary and initial conditions of the WRF~~- model~~ (3.8 version) model. The ERA5 dataset is an atmospheric reanalysis, which replaces the widely used ERA-Interim reanalysis (Berrisford et al., 2009). It has a spatial ~~grid~~resolution of 30 km with 138 vertical levels with the top at 80 km. It ~~proved~~has been shown to out perform ERA-interim in many climatological applications and as a forcing dataset for different modeling applications (Albergel et al., 2018; Tarek et al., 2019; Wang et al., 2019 among others). The parametrization schemes used in the WRF simulation include: the Thompson cloud microphysics scheme (Thompson et al., 2008), the NCAR Community Atmosphere Model (CAM) scheme for both shortwave and longwave radiations (Neale et al., 2004), the Noah-MP scheme for the land surface physics (Niu et al., 2011), the Mellor-Yamada-

Janjic scheme for the planetary boundary layer (Janjic, 2002) and the Betts-Miller-Janjic scheme (Betts and Miller, 1986; Janjic, 1994) for deep and shallow convection. This WRF configuration has ~~proved~~shown its consistency in previous studies simulating the seasonal snowpack over complex terrain (Ikeda et al., 2010; Rasmussen et al., 2011). In addition to the described parametrization, we applied the spectral nudging technique to satisfy the large scale atmospheric conditions at the higher altitudes, while allowing the model to have its own dynamics inside the planetary boundary layer (Von Storch et al., 2000; Waldron et al., 1996). The spectral nudging technique was applied for the wind vectors, temperature and geopotential with a wave number of ~~1~~one in each direction, based on the parameters recommended by Gómez and Miguez-Macho (2017), and nudging the waves above ~ 1000 km wavelength.

Next, the ICAR model was used to obtain a finer 1 km x 1 km spatial grid atmospheric simulation nested in the aforementioned WRF simulation domain. This enabled us to significantly reduce the high computational cost compared to a long-term high-resolution WRF simulation. ICAR is a 4D meso-atmospheric model designed for downscaling purposes based on linear mountain wave theory. The linear theory allows ICAR to compute the main dynamical effect of topography on the atmosphere using an analytical solution, thus avoiding the need to solve the Navier-Stokes equations and reducing computational cost by a factor of 100. The center of the ICAR simulation was established in the center of the WRF simulation, using 179 x 179 grid cells in both latitude and longitude directions and preventing the boundaries from intersecting complex terrain. The model top was situated at 4150 m above the topography with 12 vertical levels, using the default model levels heights (Horak et al., 2019). The model configuration used: the Thompson cloud microphysics scheme (Thompson et al., 2008), the Noah land surface model (Chen and Dudhia, 2001) and the Multidimensional Positive Definite Advection Transport Algorithm (MPDATA) for the advection (Smolarkiewicz and Margolin, 1998). Convection schemes were not implemented for this simulation and the radiative fluxes at the surface were prescribed by WRF. The lack of convection could have some impact on the total amount of precipitation, and therefore on the seasonal snowpack. However, such deviations in the total amount of precipitation are partly compensated by the PBS (as described in section 3.3.2).

3.2 Ensemble-based fractional snow cover assimilation

3.2.1 MODIS fractional snow cover area data estimation

For this study, we used satellite observations of fSCA, assimilated in an ensemble of snow simulations to improve the snow water equivalent products (SWE) of ICAR. The daily fSCA information was obtained by means of the MODIS sensor, which is orbiting the Earth on board two satellites, Terra and Aqua. We have chosen MODIS because of its daily revisit time combined with a spatial resolution of 500 m, which is higher than our ICAR simulation. More specifically, we have used the ~~n~~Normalized ~~d~~Difference ~~s~~Snow

~~i~~Index (NDSI) retrievals of ~~the~~ collection 6 of the NASA snow-cover products MOD10A1 (Terra) (Hall et al., 2006) and MYD10A1 (Aqua) (Hall and Riggs, 2016) distributed by the National Snow and Ice Data Center. To estimate the fSCA from the MODIS NDSI we have used a linear function following Salomonson and Appel (2004). The coefficients of the function were optimized using a serie~~s~~ of 20 m resolution snow products from Theia Snow collection~~-~~ (Gascoin et al., 2019). The Theia Snow collection provides snow cover area maps ~~that were~~ derived from Sentinel-2 observations. The revisit period of Sentinel-2 is at most 5 days since the launch of Sentinel-2B (i.e. after march 2017). It can be shorter in areas where successive swaths overlap laterally. We downloaded 645 Theia Sentinel-2 snow products acquired between 2017-09-03 and 2018-12-24 over Lebanon. For every Sentinel-2 image we can match a MODIS image since there is a MODIS image every day over Lebanon during the same period. Theia binary snow maps were resampled to 500 m fSCA in the same grid as the MODIS products by averaging the contributing pixels. By comparing these fSCA Theia maps with the MOD10A1 products we could find 5.84×10^4 cloud-free pixels which corresponded to MOD10A1 snow-covered pixels on the same date. A subset of 40% of ~~these~~the NDSI-fSCA were used to fit ~~a~~the linear function using the least squares method. The optimized function was tested against the remaining data and yielded an fSCA RMSE of 11% and a mean absolute error of 5.7%. The same analysis was done with MYD10A1 (Aqua) products but we ~~did not use them in the following~~ opted not to use them in the remainder of the analysis because ~~as~~ they exhibited a lower agreement with the Theia Sentinel-2 snow cover products (RMSE of 21%). The lower agreement of MYD10A1 is likely due to degraded ~~detectors~~sensors (Wang et al., 2012) but may also be related to the difference between the overpass time of Sentinel-2 (10:30 local time) and Aqua (13:30 local time), while Terra share the same overpass time as Sentinel-2.

We reprojected the generated MODIS fSCA products to the spheroid datum (6370 km earth radius) Lambert conformal projection used in the ICAR simulation. To avoid artifacts as consequence of the data gaps of MODIS imagery caused by the cloud cover, we have performed the aggregation when the majority of the MODIS cells used to calculate each new resampled cell was cloud free (less than 25% cloud cover), otherwise the cell was considered empty missing for the scene in question. In previous studies, the MODIS fSCA products have ~~proved~~shown to have a good performance retrieving fSCA information compared with field observations even considering its moderate resolution (Aalstad et al., 2020). Thus, they are a robust resource to use when developing regional scale snow reanalysis.

3.2.2 Particle batch smoother implementation

The assimilation procedure was implemented using the PBS scheme (Margulis et al., 2015). The PBS assigns a weight to each ensemble member according to its agreement with the observations through Bayes theorem. The most obvious advantage of this technique is its computational efficiency, as it avoids the resampling step common in

other assimilation algorithms. A complete description of the PBS can be found in Margulis et al. (2015). It is also summarized in Aalstad et al. (2018) and Fiddes et al. (2019). The PBS has been shown to perform well relative to other assimilation algorithms when used to assimilate fSCA information (Aalstad et al., 2018; Margulis et al., 2015), even though it can suffer from particle degeneracy as consequence of a highly inhomogeneous distribution of weights (Van Leeuwen, 2009). ~~T~~In this context, the PBS has been successfully used to develop a series of snowpack reanalyses (Cortés et al., 2016; Fiddes et al., 2019; Margulis et al., 2016).

For the prior of the PBS implementation, we generated an ensemble of snowpack simulations forcing the FSM2 (Essery, 2015), with the ICAR predicted surface meteorology. The configuration of the FSM2 model includes an albedo correction as snow ages with time differently for melting and cold snow, and increase~~d~~s with snowfall with a maximum of 0.9. The compaction rate was calculated based on overburden and thermal metamorphism (Verseghy, 1991). The turbulent exchange coefficient was stability corrected based on the bulk Richardson number. The thermal conductivity was calculated based on snow density. Finally, the FSM2 configuration accounted for retention and refreezing of water inside the snowpack. Such a configuration has been shown to properly simulate the inter- and intra-annual variability of the snowpack dynamics over ~~mountains~~ mountains with a similar Mediterranean climate (Alonso-González et al., 2018).

To generate the ensemble of forcing datasets, we perturbed the precipitation and the 2 m air temperature surface fields of the ICAR output using a log-normal and a normal (Gaussian) probability density functions respectively. We choose the mean of the probability functions from the averaged biases of the ICAR simulation, estimated form independent observations provided by three mountain AWS at the locations shown in Figure 1 (Fayad et al., 2017a). The variance of the probability distribution functions was calculated by ~~increasing~~doubling the variance of the errors ~~by a factor of two~~ to increase the spread of the ensemble to cover the apparent uncertainty in the ~~of~~ ICAR outputs. The precipitation phase had to be recalculated for the new synthetic temperatures for each ensemble member. Due to the strong dependency of the snowpack over Lebanon on precipitation phase, a simple temperature threshold based precipitation phase partitions are not recommended (Fayad and Gascoin, 2020). Instead, we have used the psychrometric energy balance method approach proposed by Harder and Pomeroy (2013), where the precipitation phase is estimated by means of the estimation of the temperature of the falling hydrometeor calculated form the air temperature and relative humidity. A total of 400 ensemble members per ICAR cell were independently generated by randomly drawing multiplicative time-constant parameters from the log-normal probability function for precipitation, and additive parameters from the normal probability function for the 2 m air temperature.

To estimate the fSCA of each ensemble member we used the probabilistic snow depletion curve proposed by Liston (2004). This model simulates the subgrid peak SWE distribution using a lognormal probability density function. Then, the fSCA is diagnosed using the accumulated melt depth estimated from the energy balance outputs of the FSM2, the peak mean SWE, and the peak subgrid ~~of variationcoefficient~~ coefficient of variation (CV) ~~of~~ of the lognormal probability density function, assuming a constant melt over the grid cell. ~~The coefficient of variation of the lognormal probability density function~~The CV used in this model is strongly controlled by the characteristics of the terrain. We have included th~~is~~e CV parameter as part of the assimilation, perturbing its value inside the recommended values in Liston (2004) using a mean of 0.4 and a variance of 0.01 (Aalstad et al., 2018). The PBS was implemented over the fSCA ensemble over each grid cell and season independently, using the values of the melting season, corresponding ~~with~~to the months of March through June. Finally, the generated SWE products (ICAR_assim hereafter) were estimated from the weighted mean of the SWE of the ensemble members, where the weights were obtained using the PBS. A schematic description of the whole process is presented in Figure 2.

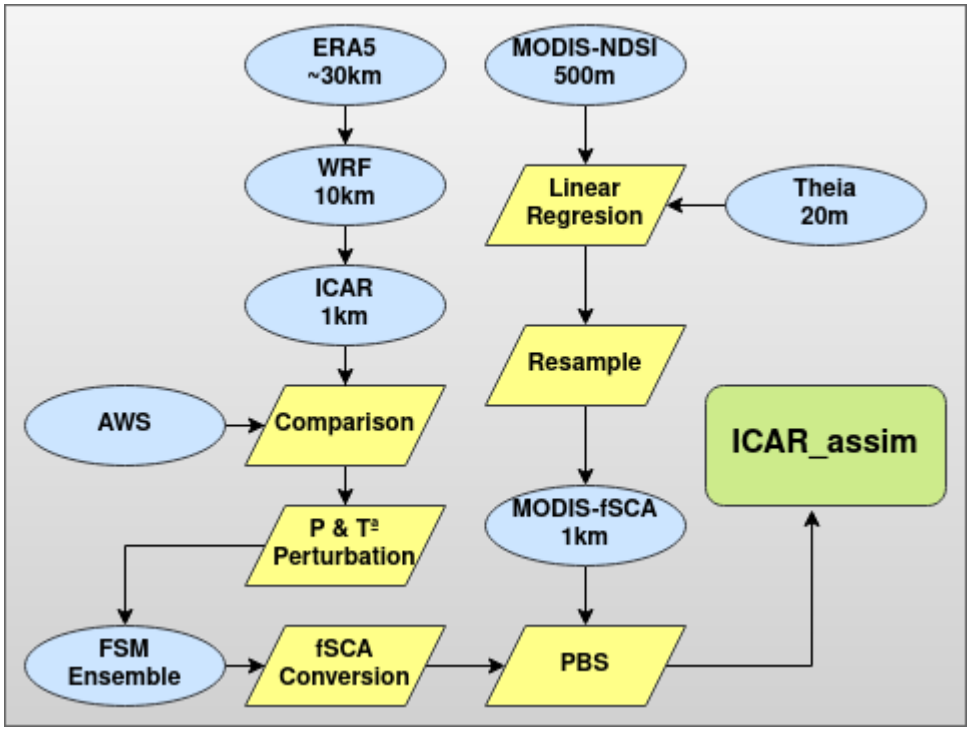

Figure 2: Schematic flow chart of the ICAR_assim snow product development

3.3 Validation procedure and analysis of the SWE products

The ICAR atmospheric simulation and the ICAR_assim products were compared against independent observations. First, the ICAR atmospheric simulation was compared with three ~~automatic weather stations (~~AWS~~)~~ located in the main mountain range of the domain (Fayad et al., 2017a)(Figure 1). Temperature and precipitation measurements were aggregated to the hourly model output frequency from the original 30-minute time resolution. Then, the temperature and precipitation biases were estimated. The precipitation data was available only in two of the AWS. The error values and its variance were used to define the shape of the probability density functions of the perturbation parameters described above to generate each ensemble.

Table 1: AWS geographical coordinates and elevations. Elevation of the ICAR cell that contains each AWS.

AWS	Snow seasons	Elevation [m a.s.l.]	Latitude (WGS84)	Longitude (WGS84)	ICAR elevation [m a.s.l.]
A	2013 to 2016	2834	34.27º N	36.09º E	2827
B	2014 to 2016	1843	34.14º N	35.88º E	1746
C	2011 to 2016	2296	33.98º N	35.86º E	2272

After the PBS implementation, we compared the ICAR and ICAR_assim snow products with the snow depth observed information of the three AWS. The observed snow depth was transformed into SWE by assuming a constant snow density value of 467 kg m^{-3}, estimated from observations in the area (Fayad et al., 2017a). That was necessary to make the AWS data comparable with the ICAR snow outputs as they are provided only as SWE. Even if it is commonly implemented in operational atmospheric forecast models, the assumption of a constant density could introduce obvious bias in the SWE estimation (Dawson et al., 2017). In the Mediterranean snowpacks, such biases are partially reduced as consequence of the high densification rates of the snowpack (Bormann et al., 2013; Fayad et al., 2017b). However, we introduced a sensitivity analysis in the comparison, varying the density value in the range of ± 15% to illustrate such uncertainity. To compensate the big shift between the ICAR and ICAR_assim resolutions (1 km x 1 km) and the point-scale nature of the AWS observations, we have interpolated a new SWE series from the 4 nearest cells of the simulations using the inverse distance method. ~~Then,~~

The spatial accuracy of the SWE products was compared ~~against~~to satellite observations. First, we developed a daily gapfilled snow cover time series covering the time period of the ICAR simulation from the MODIS snow cover products using the methodology proposed by Gascoin et al. (2015). Then, the products were aggregated to estimate the averaged snow presence over each cell in percentage (~~P(snow)~~ $P(snow)$). The MODIS

~~P(snow)~~ $P(snow)$ product was aggregated to the ICAR grid to make it comparable. Then, we calculate the ~~P(snow)~~ $P(snow)$ for the ICAR and ICAR_assim simulations. We ~~chose~~choose a SWE MODIS detection threshold of 20 mm to calculate the ~~P(snow)~~ $P(snow)$ from the simulated SWE series, inside the range recommended by Gascoin et al. (2015). All the spatial analys~~e~~is and the data assimilation was computed over the areas that had exhibited a ~~P(snow)~~ $P(snow)$ –> 5%, which amounts to a total ~~area~~surface of 4412 km^2.

4. Results and Discussion

4.1 Atmospheric simulation results

The use of ICAR is justified as it is computationally inexpensive compared to similar WRF simulations, while retaining a physical basis to enable simulations in regions lacking observations. The speed up factors can range from 140 in its more complex configurations (as choose for this study) to 800 in its simpler configurations (Gutmann et al., 2016). However, the linear theory simplification presents some limitations when predicting the motion of the atmosphere, such as interactions between waves and turbulence (Nappo, 2012) or the lack of explicit convection. Despite these limitations, ICAR has been shown to be a valuable tool for downscalling ~~proposes~~ showing a good ~~performance compared~~consistency with observations (Horak et al., 2019), as well as ~~compared~~ with fully dynamical WRF simulations (Gutmann et al., 2016). Figure ~~2~~3 shows how the ICAR model was able to improve the 2 m air temperature data, compared with the ERA5 reanalysis (ICAR mean error= 3ºC compared with 8.5ºC in ERA5). This effect is caused by the coarser ERA5 resolution, that smooths the terrain ~~causing~~leading to warm biases. This is particularly evident in the Lebanon ranges were the elevation gradient ranges from 0 to 3000 m a.s.l. in approximately 25 km (Figure 1). Despite the ~~obvious~~clear improvement in the temperature performance, the simulation is biased towards slightly higher temperatures than ~~in~~ the AWS data. However, the main temporal patterns and the magnitude of the temperature are well represented.

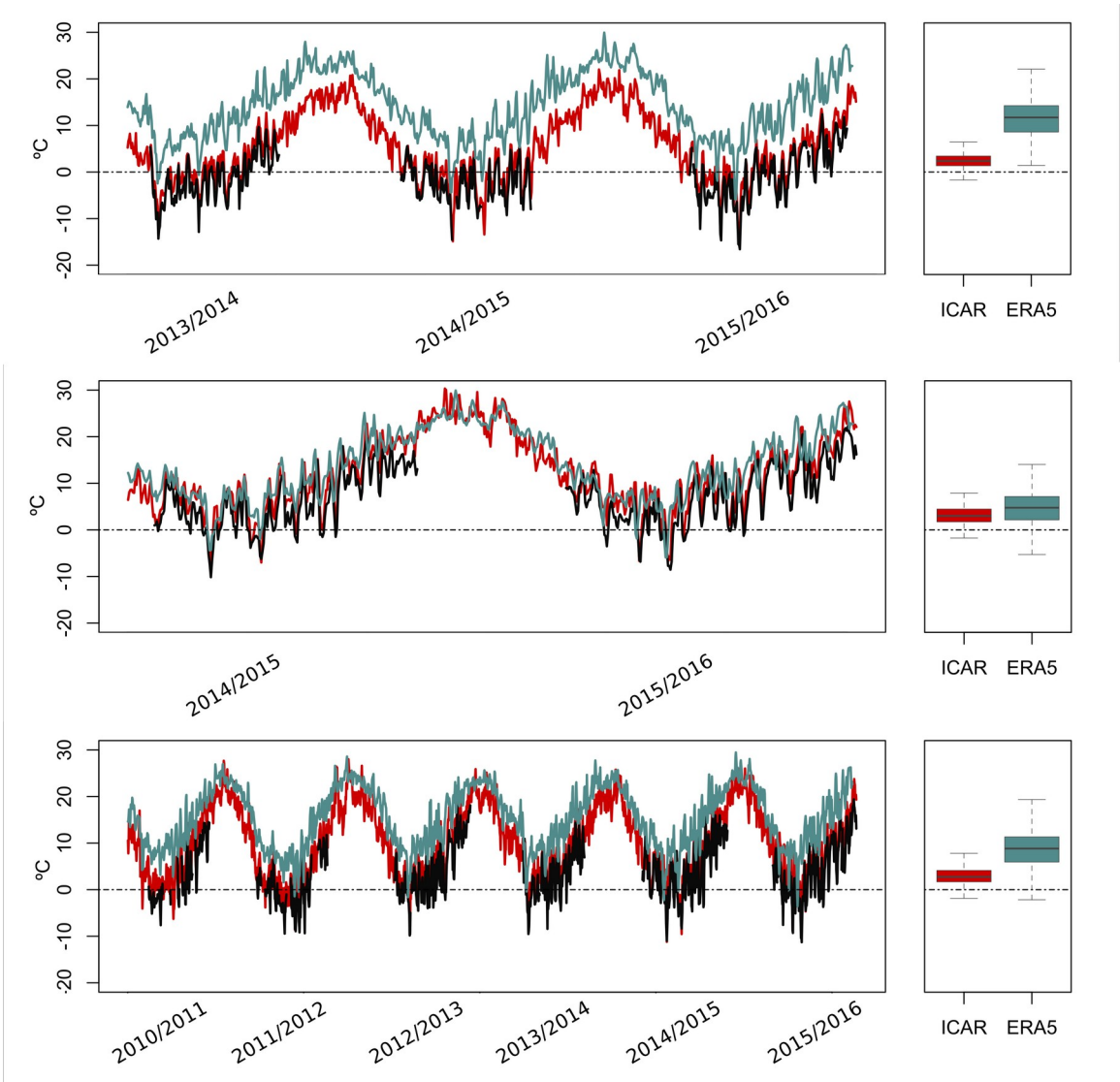

Figure 3: ERA5 (blue), ICAR (red) and AWS (black) weekly temperature data. The box-plots represent the distribution of the errors and the gray shadows the data gaps in the observations.

Similarly, precipitation outputs of ICAR were compared with the gauges deployed in two of the AWS sites. ICAR reduces the spread of the daily precipitation errors of ERA5 as shown in Figure ~~3~~4 (standard deviation of 11.5mm in ERA5 compared with the 8.4mm of ICAR), even though the ERA5 error are already surprisingly low considering the spatial resolution and the fact that precipitation is challenging to simulate by numerical models especially over complex terrain (Legates, 2014). This validation provides a range of uncertainty estimates to help generate the probability density functions for the perturbations of the ensemble. The selected parameters to define the shape of the normal

probability density function which defines the additive perturbation ~~index of~~to the temperature were set to a mean of -3.0 ºC and a variance of 1.8 ºC. Similarly, the parameters of the lognormal probability density function used to obtain the multiplicative perturbation factors for the precipitation were a mean of 2.0 and a variance of 0.75. Even though the parameters were designed to model the uncertainty of ICAR, they are similar to comparable implementations of the PBS (Cortés et al., 2016). Through the forced increase of the variance of the probability density functions, we ensure that the ensemble of snow simulations covers the expected uncertainty space of ICAR, while the PBS has proved to be robust to progressive variations of the perturbation parameters (Cortés et al., 2016).

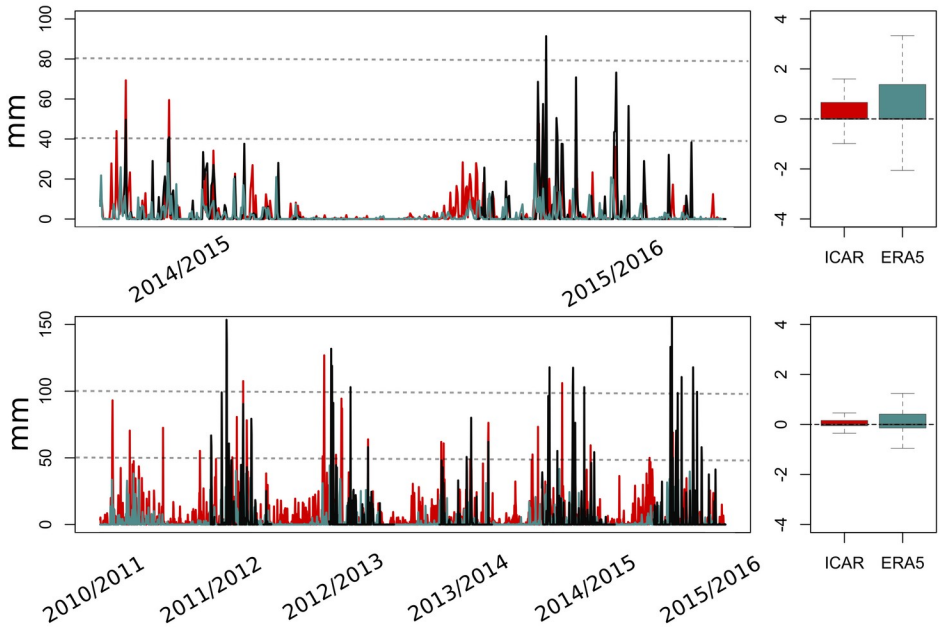

Figure 4: ERA5 (blue), ICAR (red) and AWS (black) daily precipitation data. The boxplots represent the distribution of the errors and the gray shadows the data gaps in the observations.

4.2 Fractional snow cover assimilation

The new proposed linear relationship function to derive fSCA from NDSI has improved the MODIS fSCA products when compared with the relationship function by Salomonson and Appel (2004) (Supplementary figure 1). Using the relationship function by Salomonson and Appel (2004) resulted in larger mean absolute error (MAE) (6.2% compared to 5.7%) and Root Mean Squared Error (RMSE) (12% compared to 11%). The equation of the linear fit is:

$$fSCA = 1.23 \cdot NDSI + 0.23$$

The performance of ICAR_assim was compared against snow depth measurements at the AWS locations (Figure ~~4~~5) and MODIS gapfilled products (Figures ~~5~~ 6 and ~~6~~7). In general, ICAR has a tendency to underestimate the SWE compared with ICAR_assim. This is likely related to the warm biases detected in the simulation, combined with the limitations of the snow model implemented in the Noah land surface model used by ICAR (Barlage et al., 2010). Thus, future versions of ICAR with better representations of the snow processes through the ~~use~~implementation of more complex land surface parametrizations like Noah-MP (Niu et al., 2011), as used in the parent WRF simulation, could potentially improve the accuracy of ICAR's SWE outputs (Suzuki and Zupanski, 2018). This effect could be particularly enhanced in the mild climatic conditions of Lebanon, as larger disagreements in the SWE outputs between Noah and Noah-MP occur under warm conditions (Kuribayashi et al., 2013). However, ~~the improvement of the snow representations of ICAR is obvious compared with ERA5 reanalysis as it was not able to reproduce the snowpack at all as a result of its coarse resolution.~~the improvement of the snow representations of ICAR is clear when compared with ERA5 reanalysis which was not able to reproduce the snowpack at all due to its coarse resolution.

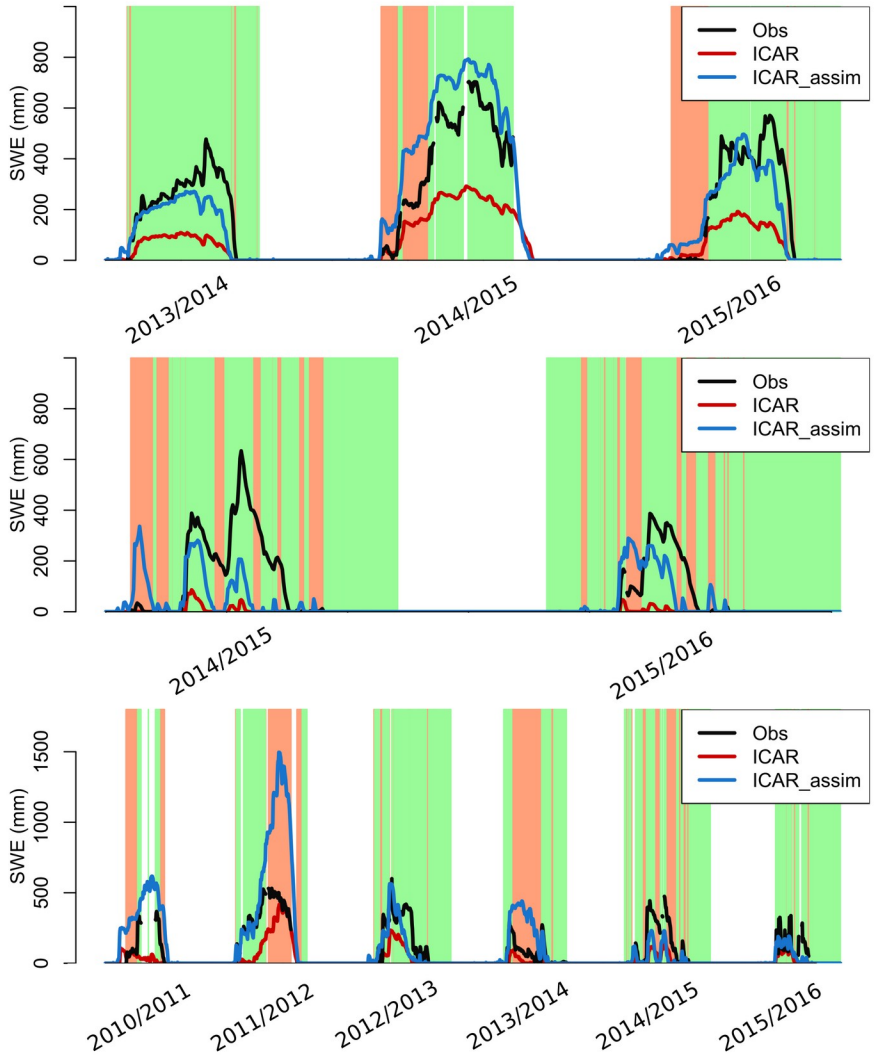

Figure 5: Comparison between observed, ICAR and ICAR_assim. SWE products. The green in the background indicates the time steps when ICAR_assim improves the performance of ICAR.

The results of the validation of ICAR_assim~~–~~ show a good agreement with the observations. For the estimated SWE, the ~~mean squared error (root~~RMSE~~)~~ and the ~~mean absolute error (~~MAE~~)~~ relative to the AWS were 189.2 mm and 104.52 mm respectively after removing the summer from the analyses, with a coefficient of correlation (R) of 0.75 for the annual mean SWE accumulation. Even though ICAR_assim generally shows a good agreement with the observations (especially considering the scale mismatch between the stations and ICAR_assim), some clear differences were found. Figure ~~4~~5 exhibits a surprisingly high difference in the magnitude of the observed SWE and the ICAR_assim output for the 2011/2012 winter season in the third AWS. However, independent observations in the area have described an exceptional snowpack ~~during the~~

~~2011/2012~~in this season, with snow depths more than 6 m even reaching up to 10 m locally (Koeniger et al., 2017). Such disagreements between the AWS information and the independent observations can be explained by the high spatial heterogeneity of the snow depth at point scales (López-Moreno et al., 2011). This effect was studied~~in depth~~ in the Atlas ~~mountains~~mountains, where the agreement of the snow simulations rapidly drops using resolutions over 250 m (Baba et al., 2019). Such spatial heterogeneity has been shown to be particularly high over mount Lebanon due to the important role of the wind redistribution as consequence of ~~-~~geomorphology (Fayad and Gascoin, 2020). For example, Fayad and Gascoin (2020), reported large differences with the AWS data from in situ measurements on 15 of January 2016, when they measured snow depths up to 258 cm on the surroundings of the third AWS location (Figure ~~4~~5; bottom panel), while the AWS sensor itself detected 7.5 cm. However, the comparison between the temporal patterns of the snow cover over Lebanon from MODIS gap-filled daily products and ICAR_assim have shown good levels of agreement with a RMSE=270.2 km^2, a MAE=124.1 km^2 over a total surface of 4412km^2 (Figure ~~5~~6), and a Pearson correlation value of R=0.88 in the annual maximum of the snow cover extent (Figure ~~5~~6). The larger spatial support of the MODIS products permits a more representative and extensive validation of ICAR_assim. Thus, the good agreement between both snow cover products and the generally ~~comparable~~ SWE magnitudes with the AWS observations shows the temporal consistency of the ICAR_assim reanalysis.

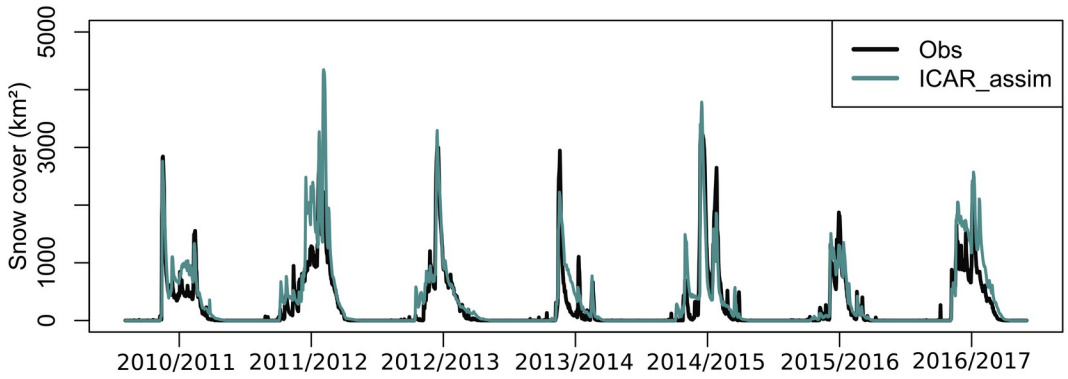

Figure 6: Daily snow cover extent comparison between MODIS gapfilled products and ICAR_assim.

The spatial patterns of ICAR_assim, were also compared with the MODIS gapfilled products (Figure 7). The spatial comparison of the ~~P(snow)~~ $P(snow)$ ~~-~~showed a very good level of agreement demostrating the potential of fSCA assimilation through the PBS in improving the ICAR SWE products. ~~with a~~ The comparison showed a correlation value of R=0.98, a RMSE=3.0 % and a MAE=2.3 % improving the ICAR simulation that exhibited values of R=0.79, RMSE=14.3% and MAE=12.3%. There was a general

tendency to slightly underestimate the ~~$P_{(snow)}$~~ $P(snow)$ values by ICAR_assim, specially at the lower elevations. We hypothesize that this effect could be caused by the selection of a constant SWE depth to calculate the snow cover from the ICAR_assim product. Thus, the shallow snowpacks whose SWE values are under the selected threshold are not recorded as snow presence in the ICAR_assim even though they could potentially be detected as snow by the MODIS sensor. In addition, the MODIS snow cover products should be considered less accurate over areas of ~~fast~~ ~~melting~~rapid melt (Gascoin et al., 2015). Such mismatch between ICAR_assim and MODIS combined with the fact that the 2011 – 2012 snow season showed persistent cloud covers related with its exceptional snowpack, could explain the biases in the Figure 6. During the 2011 – 2012 snow season, the gapfilling algorithm had less information to fill the MODIS snow cover time series, while the PBS had propagated the fSCA information through the whole season from the few available observations. In summary, our results have shown how ICAR_assim can accurately reproduce the inter-annual and intr-annual spatiotemporal patterns of the snow cover, with a SWE magnitude comparable with independent observations that agree well in ~~its~~terms of temporal patterns.

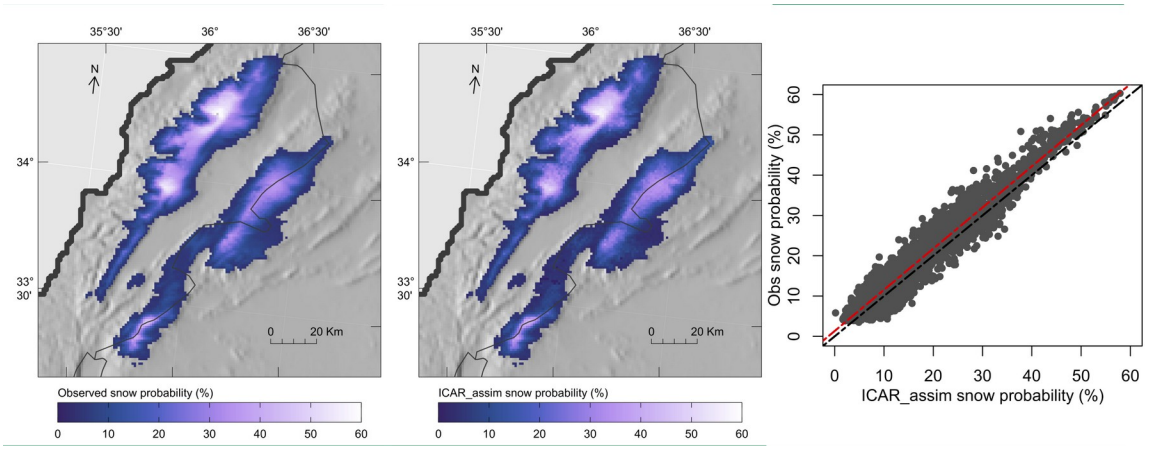

Figure 7: Snow probability spatial comparison between observed MODIS products and ICAR_assim.

4.3 Snowpack dynamics over Lebanon ~~mountains~~mountains

ICAR_assim exhibits some limitations that should be considered. First, despite the high resolution of the reanalysis the regional nature of the simulations prevent the representation of some processes like wind or avalanches snow redistribution. In addition, there are some other sources of uncertainty involved in the development of the reanalysis, like the depletion curve, the fSCA derived from MODIS or the structural uncertainty associated with each model. However, ICAR_assim has been shown to be

consistent with the limited observations providing a valuable resource in the data scarce context of the Lebanese mountains.

Figure ~~7~~8 shows the spatial distribution of the mean peak SWE values and its temporal coefficient of variation for the 2010-2017 time period~~reecent years~~. Such values can be influenced by the fact that the study period is relatively humid compared with the previous years (Cook et al., 2016), showing slightly higher values than a long term climatology. However, the length of the reanalyses constitutes a reasonably representative sample of the main snowpack dynamics over the region~~-~~. The snowpack over Lebanon has exhibited the high temporal variability that is characteristic of the Mediterranean snowpacks (Fayad et al., 2017b), with similar values of the coefficient of variation as those observed ~~on~~in other Mediterranean mountain ranges (Alonso-González et al., 2020). The maximum accumulations reach 2000 mm of SWE and are located at the higher elevations of mount Lebanon, where there is a plateau over the elevation of the winter zero isotherm (Fayad and Gascoin, 2020). The temporal coefficient of variation of the annual peak SWE follows unequal spatial patterns~~,~~. . It ~~tending~~tends to exhibit higher values over the areas sheltered from direct ~~intereaction~~interaction with the warm and moist Mediterranean air. ~~i~~In addition it exhibits ~~to~~ a decreasing trend with elevation (Figure ~~8~~9) as found in other Mediterranean ranges (Alonso-González et al., 2020), reaching a mimimum of 15%.

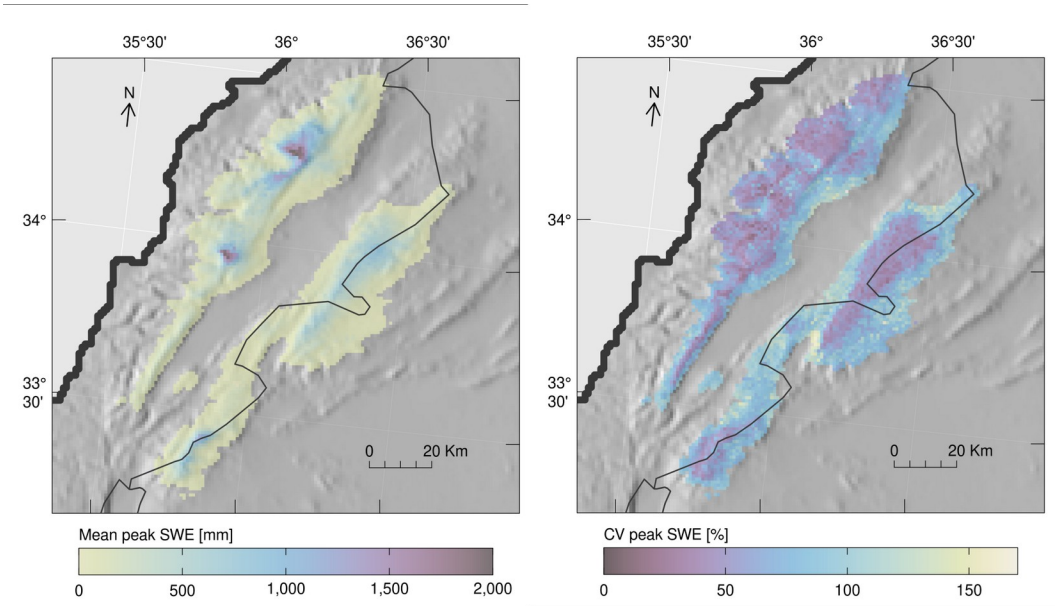

Figure 8: Averaged annual peak SWE (left) and annual coefficient of variation (right).

There are ~~obvious~~clear differences between the Lebanon and Anti-Lebanon ranges, that can be just partially explained by their different orography. Despite the closeness of both Lebanon and Anti-Lebanon ranges, they exhibit different relationships between the values of mean peak SWE (Figure ~~8~~9 top panel) and snow duration(~~–~~Figure ~~8~~9 bottom panel) and~~–~~ with the elevation, showing that the differences are not just related to the particular orography of each range, but also with its climatological characteristics. Thus, at comparable elevations mount Lebanon tends to show higher values of ~~–P(snow)~~ $P(snow)$ ~~_~~and mean peak SWE, with lower values of coefficient of variation, suggesting thicker, longer lasting and seasonally ~~ensured~~stable snowpack. The orographic precipitation caused by the uplift of the Mediterranean moisture is a major source of precipitation in the area (Jomaa et al., 2019)~~,~~ ~~t~~That is probably why Anti-Lebanon ~~mountains~~mountains shows lower peak accumulations than Mount Lebanon, with Anti-lebanon in the rain shadow leading to lower precipitation and snow accumulation. However, despite the differences in the coefficient of variation values, they tend to become similar at the higher elevations. The same coefficient of variation occurs in the elevations where the precipitation leads the snow accumulation while they differ at the lower elevations, where the accumulation is conditioned by the temperature. This effect suggest warmer conditions on the Anti-Lebanon mountain as consequence of leeside wind effects (Foëhn type effect), and confirm the sensitivity of the snow simulation to the chosen partition phase method over Mediterranean ~~mountains~~mountains (Fayad and Gascoin, 2020).

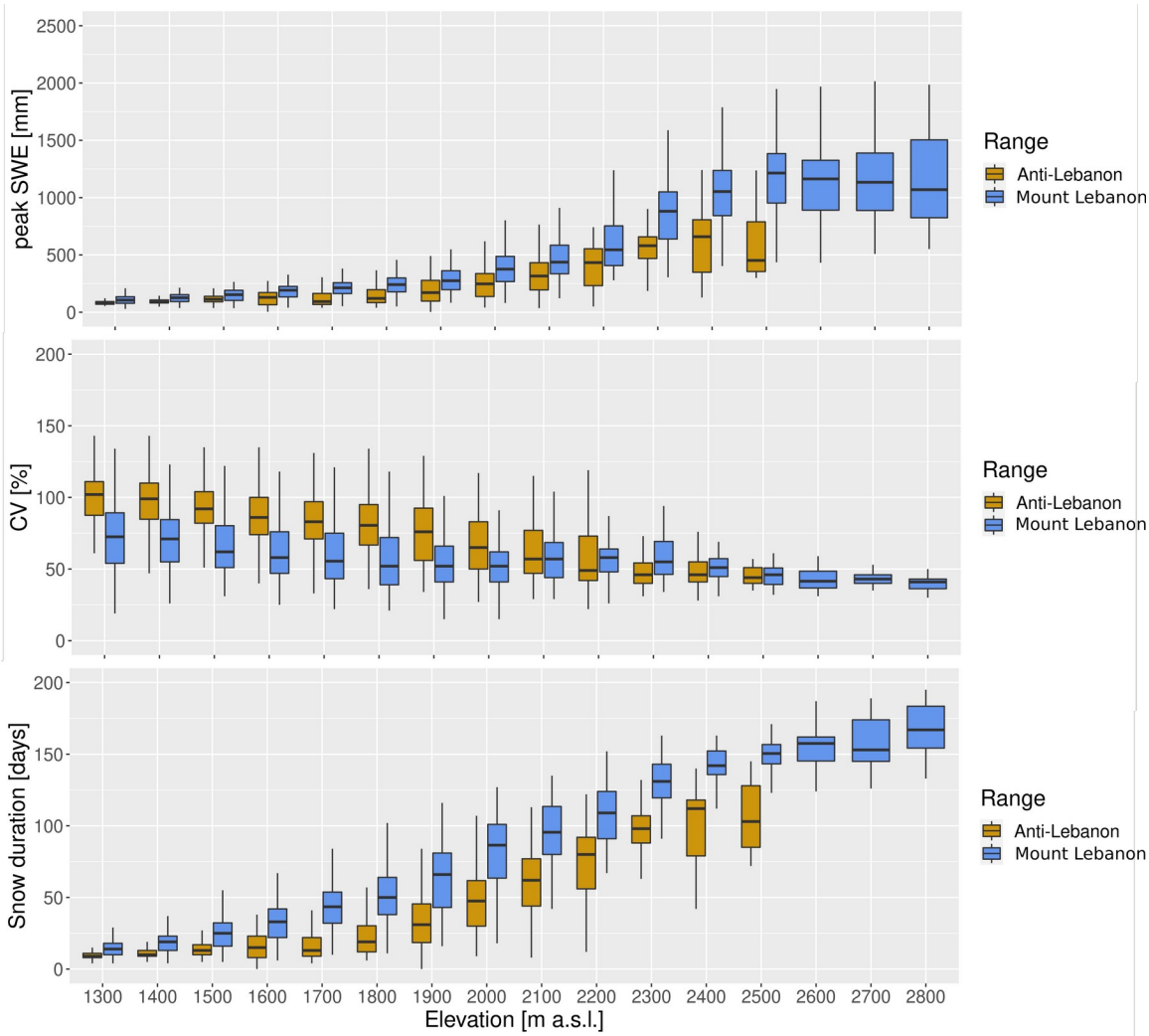

Figure 9: Relationship between annual peak SWE and elevation (top), coefficient of variation and elevation (middle), and snow duration and elevation (bottom).

Figure 910 shows the averaged seasonal SWE accumulation at different elevations over both the Lebanon and Anti-Lebanon ranges. Each elevation represents the aggregated pixels of the elevation with a range of ± 50 m a.s.l. For reference, they show on average a peak SWE of 306 mm at the elevation band of 2000 m a.s.l., which is comparable to those found in the Iberian Peninsula mountain ranges (Alonso-González et al., 2020). More specifically, the peak SWE and duration values shows intermediate values between the Central Iberian and Pyrenees ranges at 2000 m a.s.l, but with a peak SWE coefficient of variation of 53 %, that is greater than the highest values of Iberia located at Sierra Nevada with 34 %. The relative area lying at each elevation compared with the total elevation over 1300 m a.s.l. is represented to highlight the importance of the hypsography from the hydrological point of view. Thus, Lebanon exhibits a deep and long lasting

snowpack with up to 1000 mm of peak SWE on average particularly over 2500 m a.s.l., but the relative areal coverage of such elevations is very low. This suggest that the mean

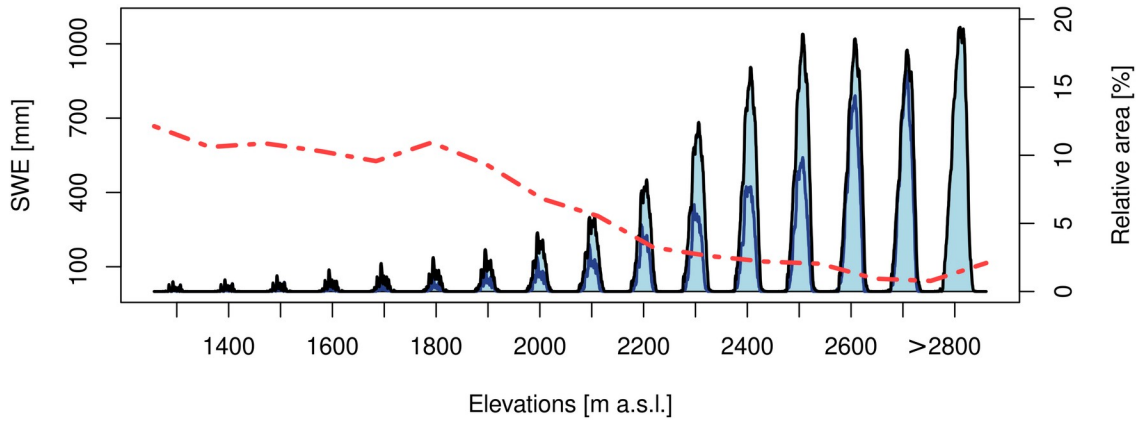

Figure 10: Mean annual evolution of SWE at different elevation bands. Dark blue line represent the Anti-lebanon range, black line the Mount Lebanon range, and red line the relative areal coverage of each elevation above 1300 m a.s.l.

peak SWE series at lower elevations could hide a large variation in mass due to the wider areas at lower elevations where many different peak SWE values can coexist, as Alonso-González et al.(2020) found in the Iberian mountain ranges.

The thick snowpacks found at the higher elevations are not necessarily the biggest fresh water resources available due to the hypsometry of the mountain area. Figure 1~~0~~1 shows ~~about~~ the average amount of freshwater stored in the snowpack per elevations band. It is obvious that the maximum amount of freshwater is stored between 2100 to 2500 m.a.s.l., despite the fact that thicker snowpacks are at higher elevations. The cumulative water storage in the snowpack is more than double in the medium elevation zone (average maximum up to 520 Hm^3 from 1300 to 2300m a.s.l.) when compared to the higher areas (average maximum up to 201 Hm^3 at 2400 m a.s.l. and onward)~~, been~~. This is ~~-~~an important part of the yearly water budget, as mean annual precipitation was estimated in to be 7200 Hm^3 for the period (2010-2016) (Jaafar et al., 2020). Noting that this in contrast to the fact that the orography of Lebanon encourages the storage of snow in the upper areas because of the existence of a high elevation plateau ~~This result suggests new challenges on the water management of Lebanon in the future as a consequence of climate warming. The snowpack at low elevation areas is more sensitive to warming (Fayad et al., 2017a; Fayad and Gascoin, 2020).~~(Fayad et al., 2017a; Fayad and Gascoin, 2020). These results suggest new challenges for the water management of Lebanon in the future as a consequence of warming climate. The snowpack at low elevation areas is more sensitive to warming (Jefferson, 2011; Marty et al., 2017; Sproles et al., 2013), particularly over areas with mild winter conditions as has been shown in other Mediterranean regions (Alonso-González et al., 2020a).

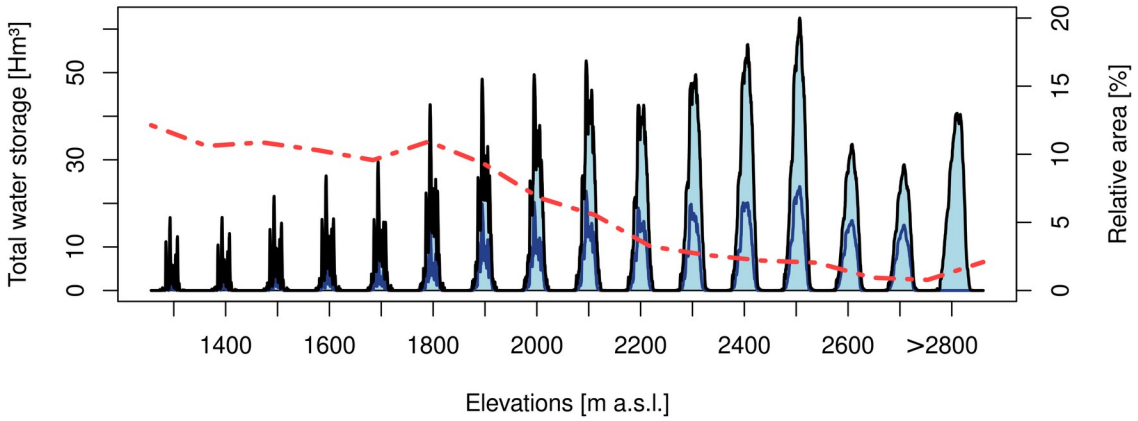

Figure 11: Averaged annual water stored in the snowpack at different elevation bands. Dark blue line represent the Anti-Lebanon range, black line the total stored in Lebanon, and red line the relative areal coverage of each elevation above 1300 m a.s.l.

45. Conclusions

The assimilation of MODIS fSCA through the use of the PBS has proven to be a cost effective way to use remote sensing data in snow simulations, and is particularly appropriate for simulating snow in data scarce regions. Thus, the generated SWE products show good agreement with MODIS snow cover gapfilled data, with R = 0.98, RMSE = 3.0 % and MAE = 2.3 % for the spatial map of the probability of snow. The time series of snow cover showed a R=0.88, RMSE=270.2 km^2, and MAE=124.1 km^2 over a total surface of 4412km^2. The performances in terms of SWE magnitude with the few available point-scale observations ~~with~~was R=0.75, RMSE=189.2 mm, and MAE = 104.5 mm after removing the summer from the analyses.

The snowpack over Lebanon is characterized by a high temporal variability. Some differences exist between its two main mountain ranges. ~~Thus,~~ Mount Lebanon exhibits thicker, longer and more regular snowpacks compared to the Anti-Lebanon range. Such differences cannot only be explained by the elevation difference but also reflects the dryer conditions on the leeside of the Mount Lebanon range due the rain shadow effect. The hypsometry of Lebanon results in the most important snow freshwater reservoir being in the middle elevations (2200-2500 m a.s.l.). Snowpacks at these elevations close to the 0 ºC isotherm are highly vulnerable to climate warming. As such, our findings suggest big challenges for the future management of water resources over the Lebanon region.

Acknowledgments: Esteban Alonso-González is supported by the Spanish Ministry of Economy and Competitiveness (BES-2015-071466). This study was funded by the Spanish Ministryof Economy and Competitiveness projects CGL2014-52599-P10 (IBERNIEVE) and CGL2017-82216-R (HIDROIBERNIEVE). We acknowledge support of the publication fee by the CSIC Open Access Publication Support Initiative through its

Unit of Information Resources for Research (URICI). Kristoffer Aalstad was funded by the Satperm project (239918; Research Council of Norway), a Personal Overseas Research Grant (Research Council of Norway), and the European Space Agency Permafrost CCI project (http://cci.esa.int/Permafrost), and acknowledges support from the LATICE strategic research area at the University of Oslo.

Code and data availability: WRF code can be downloaded from https://www2.mmm.ucar.edu/wrf/users/downloads.html. ICAR code can be found at https://github.com/NCAR/icar. FSM2 is archived at https://github.com/RichardEssery/FSM2. The meteorological data can be found at https://doi.org/10.5281/zenodo.583733.

Author Contribution: EAG: Conceptualization, Methodology, Writing – original draft, Software, Data curation, Validation, Visualization. EG: Methodology, Software, Supervision, Writing – review & editing. KA: Conceptualization, Methodology, Software, Writing – review & editing. AF: Methodology, Conceptualization, Writing – review & editing. MB: Data curation, Software, Writing – review SG: Conceptualization, Data curation, Methodology, Supervision, Writing – review & editing.

Conflicts of Interest: The authors declare no conflict of interest in this article

References

Aalstad, K., Westermann, S., Bertino, L., 2020. Evaluating satellite retrieved fractional snow-covered area at a high-Arctic site using terrestrial photography. Remote Sens. Environ. 239, 111618. https://doi.org/10.1016/j.rse.2019.111618

Aalstad, K., Westermann, S., Schuler, T.V., Boike, J., Bertino, L., 2018. Ensemble-based assimilation of fractional snow-covered area satellite retrievals to estimate the snow distribution at Arctic sites. Cryosphere 12, 247–270. https://doi.org/10.5194/tc-12-247-2018

Albergel, C., Dutra, E., Munier, S., Calvet, J.C., Munoz-Sabater, J., De Rosnay, P., Balsamo, G., 2018. ERA-5 and ERA-Interim driven ISBA land surface model simulations: Which one performs better? Hydrol. Earth Syst. Sci. 22, 3515–3532. https://doi.org/10.5194/hess-22-3515-2018

Alonso-González, E., Ignacio López-Moreno, J., Gascoin, S., García-Valdecasas Ojeda, M., Sanmiguel-Vallelado, A., Navarro-Serrano, F., Revuelto, J., Ceballos, A., Esteban-Parra, M.J., Essery, R., 2018. Daily gridded datasets of snow depth and snow water equivalent for the Iberian Peninsula from 1980 to 2014. Earth Syst. Sci. Data 10, 303–315. https://doi.org/10.5194/essd-10-303-2018

Alonso-González, E., López-Moreno, J.I., Navarro-Serrano, F., Sanmiguel-Vallelado, A., Aznárez-Balta, M., Revuelto, J., Ceballos, A., 2020. Snowpack sensitivity to temperature, precipitation, and solar radiation variability over an elevational gradient in the Iberian mountains. Atmos. Res. 243, 104973. https://doi.org/10.1016/j.atmosres.2020.104973

Alonso-González, Esteban, López-Moreno, J.I., Navarro-Serrano, F., Sanmiguel-Vallelado, A., Revuelto, J., Domínguez-Castro, F., Ceballos, A., 2020. Snow climatology for the mountains in the Iberian Peninsula using satellite imagery and simulations with dynamically downscaled reanalysis data. Int. J. Climatol. 40, 477–491. https://doi.org/10.1002/joc.6223

Arasa, R., Porras, I., Domingo-Dalmau, A., Picanyol, M., Codina, B., González, M.Á., Piñón, J., 2016. Defining a Standard Methodology to Obtain Optimum WRF Configuration for Operational Forecast: Application over the Port of Huelva (Southern Spain). Atmos. Clim. Sci. 06, 329–350. https://doi.org/10.4236/acs.2016.62028

Baba, M.W., Gascoin, S., Hanich, L., 2018a. Assimilation of Sentinel-2 data into a snowpack model in the High Atlas of Morocco. Remote Sens. 10, 1982. https://doi.org/10.3390/rs10121982

Baba, M.W., Gascoin, S., Jarlan, L., Simonneaux, V., Hanich, L., 2018b. Variations of the snow water equivalent in the ourika catchment (Morocco) over 2000-2018 using downscaled MERRA-2 data. Water (Switzerland) 10, 1120. https://doi.org/10.3390/w10091120

Baba, M.W., Gascoin, S., Kinnard, C., Marchane, A., Hanich, L., 2019. Effect of Digital Elevation Model Resolution on the Simulation of the Snow Cover Evolution in the High Atlas. Water Resour. Res. 55, 5360–5378. https://doi.org/10.1029/2018WR023789

Bakalowicz, M., El Hakim, M., El-Hajj, A., 2008. Karst groundwater resources in the countries of eastern Mediterranean: The example of Lebanon. Environ. Geol. 54, 597–604. https://doi.org/10.1007/s00254-007-0854-z

Barlage, M., Chen, F., Tewari, M., Ikeda, K., Gochis, D., Dudhia, J., Rasmussen, R., Livneh, B., Ek, M., Mitchell, K., 2010. Noah land surface model modifications to improve snowpack prediction in the Colorado Rocky Mountains. J. Geophys. Res. Atmos. 115. https://doi.org/10.1029/2009JD013470

Berrisford, P., Dee, D., Poli, P., Brugge, R., Fielding, K., Fuentes, M., Kallberg, P., Kobayashi, S., Uppala, S., Simmons, A., 2009. The ERA-Interim Archive Version 2.0. ERA Rep. Ser.

Betts, A.K., Miller, M.J., 1986. A new convective adjustment scheme. Part II: Single column tests using GATE wave, BOMEX, ATEX and arctic air-mass data sets. Q. J. R. Meteorol. Soc. 112, 693–709. https://doi.org/10.1002/qj.49711247308

Bormann, K.J., Westra, S., Evans, J.P., McCabe, M.F., 2013. Spatial and temporal variability in seasonal snow density. J. Hydrol. 484, 63–73. https://doi.org/10.1016/j.jhydrol.2013.01.032

Chen, F., Dudhia, J., 2001. Coupling an advanced land surface-hydrology model with the Penn-State-NCAR MM5 modeling system. Part II: Preliminary model validation. Mon. Weather Rev. 129, 587–604. https://doi.org/10.1175/1520-0493(2001)129<0587:CAALSH>2.0.CO;2

Cluzet, B., Lafaysse, M., Cosme, E., Albergel, C., Meunier, L.-F., Dumont, M., 2020. CrocO_v1.0 : a Particle Filter to assimilate snowpack observations in a spatialised framework. Geosci. Model Dev. Discuss. 2020, 1–36. https://doi.org/10.5194/gmd-2020-130

Cook, B.I., Anchukaitis, K.J., Touchan, R., Meko, D.M., Cook, E.R., 2016. Spatiotemporal drought variability in the mediterranean over the last 900 years. J. Geophys. Res. 121, 2060–2074. https://doi.org/10.1002/2015JD023929

Cortés, G., Girotto, M., Margulis, S., 2016. Snow process estimation over the extratropical Andes using a data assimilation framework integrating MERRA data and Landsat imagery. Water Resour. Res. 52, 2582–2600. https://doi.org/10.1002/2015WR018376

Dawson, N., Broxton, P., Zeng, X., 2017. A new snow density parameterization for land data initialization. J. Hydrometeorol. 18, 197–207. https://doi.org/10.1175/JHM-D-16-0166.1

El-Fadel, M., Zeinati, M., Jamali, D., 2000. Water resources in Lebanon: Characterization, water balance and constraints. Int. J. Water Resour. Dev. 16, 615–638. https://doi.org/10.1080/713672540

Essery, R., 2015. A factorial snowpack model (FSM 1.0). Geosci. Model Dev. 8, 3867–3876. https://doi.org/10.5194/gmd-8-3867-2015

Farajalla, N., Ziade, R., Bachour, R., 2011. Drought Frequency and Evapotranspiration Trends under a Changing Climate in the Eastern Mediterranean, in: Water Scarcity and Policy in the Middle East and Mediterranean. p. 11653. https://doi.org/10.1002/aur.1388

Fayad, A., Gascoin, S., 2020. The role of liquid water percolation representation in estimating snow water equivalent in a Mediterranean mountain region (Mount Lebanon). Hydrol. Earth Syst. Sci. 24, 1527–1542. https://doi.org/10.5194/hess-24-1527-2020

Fayad, A., Gascoin, S., Faour, G., Fanise, P., Drapeau, L., Somma, J., Fadel, A., Al Bitar, A., Escadafal, R., 2017a. Snow observations in Mount Lebanon (2011-2016). Earth Syst. Sci. Data 9, 573–587. https://doi.org/10.5194/essd-9-573-2017

Fayad, A., Gascoin, S., Faour, G., López-Moreno, J.I., Drapeau, L., Page, M. Le, Escadafal, R., 2017b. Snow hydrology in Mediterranean mountain regions: A review. J. Hydrol. 551, 374–396. https://doi.org/10.1016/j.jhydrol.2017.05.063

Fiddes, J., Aalstad, K., Westermann, S., 2019. Hyper-resolution ensemble-based snow reanalysis in mountain regions using clustering. Hydrol. Earth Syst. Sci. 23, 4717–4736. https://doi.org/10.5194/hess-23-4717-2019

Fiddes, J., Gruber, S., 2014. TopoSCALE v.1.0: Downscaling gridded climate data in complex terrain. Geosci. Model Dev. 7, 387–405. https://doi.org/10.5194/gmd-7-387-2014

García-Ruiz, J.M., López-Moreno, I.I., Vicente-Serrano, S.M., Lasanta-Martínez, T., Beguería, S., 2011. Mediterranean water resources in a global change scenario. Earth-Science Rev. 105, 121–139. https://doi.org/10.1016/j.earscirev.2011.01.006

Gascoin, S., Grizonnet, M., Bouchet, M., Salgues, G., Hagolle, O., 2019. Theia Snow collection: High-resolution operational snow cover maps from Sentinel-2 and Landsat-8 data. Earth Syst. Sci. Data 11, 493–514. https://doi.org/10.5194/essd-11-493-2019

Gascoin, S., Hagolle, O., Huc, M., Jarlan, L., Dejoux, J.F., Szczypta, C., Marti, R., Sánchez, R., 2015. A snow cover climatology for the Pyrenees from MODIS snow products. Hydrol. Earth Syst. Sci. 19, 2337–2351. https://doi.org/10.5194/hess-19-2337-2015

Gómez, B., Miguez-Macho, G., 2017. The impact of wave number selection and spin-up time in spectral nudging. Q. J. R. Meteorol. Soc. 143, 1772–1786. https://doi.org/10.1002/qj.3032

Gutmann, E., Barstad, I., Clark, M., Arnold, J., Rasmussen, R., 2016. The Intermediate Complexity Atmospheric Research model (ICAR). J. Hydrometeorol. 17, 957–973. https://doi.org/10.1175/JHM-D-15-0155.1

Gutmann, E.D., Rasmussen, R.M., Liu, C., Ikeda, K., Gochis, D.J., Clark, M.P., Dudhia, J., Thompson, G., 2012. A comparison of statistical and dynamical downscaling of winter precipitation over complex terrain. J. Clim. 25, 262–281. https://doi.org/10.1175/2011JCLI4109.1

Hall, D.K., Riggs, G.A., 2016. MODIS/Aqua Snow Cover Daily L3 Global 500m SIN Grid, Version 6. NASA Natl. Snow Ice Data Cent. Distrib. Act. Arch. Center. Boulder, Color. USA. https://doi.org/https://doi.org/10.5067/MODIS/MYD10A1.006.

Hall, D.K., Riggs, G.A., Salomonson, V. V, 2006. MODIS/Terra Snow Cover 8-day L3 Global 500m Grid V005. Color. USA Natl. Snow Ice Data Cent.

Harder, P., Pomeroy, J., 2013. Estimating precipitation phase using a psychrometric energy balance method. Hydrol. Process. 27, 1901–1914. https://doi.org/10.1002/hyp.9799

Herrero, J., Polo, M.J., Eugster, W., 2016. Evaposublimation from the snow in the Mediterranean mountains of Sierra Nevada (Spain). Cryosphere 10.

Hersbach, H., 2016. The ERA5 Atmospheric Reanalysis., in: Agufm. pp. NG33D-01.

Horak, J., Hofer, M., Maussion, F., Gutmann, E., Gohm, A., Rotach, M.W., 2019. Assessing the added value of the Intermediate Complexity Atmospheric Research (ICAR) model for precipitation in complex topography. Hydrol. Earth Syst. Sci. 23, 2715–2734. https://doi.org/10.5194/hess-23-2715-2019

Ikeda, K., Rasmussen, R., Liu, C., Gochis, D., Yates, D., Chen, F., Tewari, M., Barlage, M., Dudhia, J., Miller, K., Arsenault, K., Grubišić, V., Thompson, G., Guttman, E.,

2010. Simulation of seasonal snowfall over Colorado. Atmos. Res. 97, 462–477. https://doi.org/10.1016/j.atmosres.2010.04.010

Jaafar, H., Ahmad, F., Holtmeier, L., King-Okumu, C., 2020. Refugees, water balance, and water stress: Lessons learned from Lebanon. Ambio 49, 1179–1193. https://doi.org/10.1007/s13280-019-01272-0

Janjic, Z., 2002. Nonsingular Implementation of the Mellor-Yamada Level 2.5 Scheme in the NCEP Meso model. NCEP Off. Note 437, 61.

Janjic, Z.I., 1994. The step-mountain eta coordinate model: further developments of the convection, viscous sublayer, and turbulence closure schemes. Mon. Weather Rev. 122, 927–945. https://doi.org/10.1175/1520-0493(1994)122<0927:TSMECM>2.0.CO;2

Jefferson, A.J., 2011. Seasonal versus transient snow and the elevation dependence of climate sensitivity in maritime mountainous regions. Geophys. Res. Lett. 38, n/a-n/a. https://doi.org/10.1029/2011GL048346

Jomaa, I., Saab, M.T.A., Skaf, S., El Haj, N., Massaad, R., 2019. Variability in Spatial Distribution of Precipitation Overall Rugged Topography of Lebanon, Using TRMM Images. Atmos. Clim. Sci. 09, 369–380. https://doi.org/10.4236/acs.2019.93026

Koeniger, P., Margane, A., Abi-Rizk, J., Himmelsbach, T., 2017. Stable isotope-based mean catchment altitudes of springs in the Lebanon Mountains. Hydrol. Process. 31, 3708–3718. https://doi.org/10.1002/hyp.11291

Kuribayashi, M., Noh, N.J., Saitoh, T.M., Tamagawa, I., Wakazuki, Y., Muraoka, H., 2013. Comparison of snow water equivalent estimated in central Japan by high-resolution simulations using different land-surface models. Sci. Online Lett. Atmos. 9, 148–152. https://doi.org/10.2151/sola.2013-033

Legates, D., 2014. Climate models and their simulation of precipitation. Energy Environ. 25, 1163–1175. https://doi.org/10.1260/0958-305X.25.6-7.1163

Liston, G.E., 2004. Representing subgrid snow cover heterogeneities in regional and global models. J. Clim. 17, 1381–1397. https://doi.org/10.1175/1520-0442(2004)017<1381:RSSCHI>2.0.CO;2

Liston, G.E., Elder, K., 2006. A distributed snow-evolution modeling system (snowmodel). J. Hydrometeorol. 7, 1259–1276. https://doi.org/10.1175/JHM548.1

López-Moreno, J.I., Fassnacht, S.R., Beguería, S., Latron, J.B.P., 2011. Variability of snow depth at the plot scale: Implications for mean depth estimation and sampling strategies. Cryosphere 5, 617–629. https://doi.org/10.5194/tc-5-617-2011

López-Moreno, J.I., García-Ruiz, J.M., 2004. Influence of snow accumulation and snowmelt on streamflow in the central Spanish Pyrenees / Influence de l'accumulation et de la fonte de la neige sur les écoulements dans les Pyrénées centrales espagnoles. Hydrol. Sci. J. 49. https://doi.org/10.1623/hysj.49.5.787.55135

López-Moreno, J.I., Gascoin, S., Herrero, J., Sproles, E.A., Pons, M., Alonso-González, E., Hanich, L., Boudhar, A., Musselman, K.N., Molotch, N.P., Sickman, J., Pomeroy, J., 2017. Different sensitivities of snowpacks to warming in Mediterranean climate mountain areas. Environ. Res. Lett. 12. https://doi.org/10.1088/1748-9326/aa70cb

Lundquist, J., Hughes, M., Gutmann, E., Kapnick, S., 2019. Our skill in modeling mountain rain and snow is bypassing the skill of our observational networks. Bull. Am. Meteorol. Soc. 100, 2473–2490. https://doi.org/10.1175/BAMS-D-19-0001.1

Margulis, S.A., Cortés, G., Girotto, M., Durand, M., 2016. A landsat-era Sierra Nevada snow reanalysis (1985-2015). J. Hydrometeorol. 17, 1203–1221. https://doi.org/10.1175/JHM-D-15-0177.1

Margulis, S.A., Girotto, M., Cortés, G., Durand, M., 2015. A particle batch smoother approach to snow water equivalent estimation. J. Hydrometeorol. 16, 1752–1772. https://doi.org/10.1175/JHM-D-14-0177.1

Marty, C., Schlögl, S., Bavay, M., Lehning, M., 2017. How much can we save? Impact of different emission scenarios on future snow cover in the Alps. Cryosphere 11, 517–529. https://doi.org/10.5194/tc-11-517-2017

Mernild, S.H., Liston, G.E., Hiemstra, C.A., Malmros, J.K., Yde, J.C., McPhee, J., 2017. The Andes Cordillera. Part I: snow distribution, properties, and trends (1979–2014). Int. J. Climatol. 37, 1680–1698. https://doi.org/10.1002/joc.4804

Mhawej, M., Faour, G., Fayad, A., Shaban, A., 2014. Towards an enhanced method to map snow cover areas and derive snow-water equivalent in Lebanon. J. Hydrol. 513, 274–282. https://doi.org/10.1016/j.jhydrol.2014.03.058

Montavez, J.P., Lopez-Romero, J.M., Jerez, S., Gomez-Navarro, J.J., Jimenez-Guerrero, P., 2017. How much spin-up period is really necessary in regional climate simula-

tions?, in: Geophysical Research Abstracts EGU General Assembly. Vienna, Austria, pp. 2017–15806.

Nappo, C.J., 2012. The Linear Theory, 2nd ed, International Geophysics. Academic Press. https://doi.org/10.1016/B978-0-12-385223-6.00002-1

Neale, R.B., Chen, C., Lauritzen, P.H., Williamson, D.L., Conley, A.J., Smith, A.K., Mills, M., Morrison, H., 2004. Description of the NCAR Community Atmosphere Model (CAM 5 . 0). Ncar/Tn-464+Str 214. https://doi.org/10.5065/D63N21CH

Niu, G.Y., Yang, Z.L., Mitchell, K.E., Chen, F., Ek, M.B., Barlage, M., Kumar, A., Manning, K., Niyogi, D., Rosero, E., Tewari, M., Xia, Y., 2011. The community Noah land surface model with multiparameterization options (Noah-MP): 1. Model description and evaluation with local-scale measurements. J. Geophys. Res. Atmos. 116, D12109. https://doi.org/10.1029/2010JD015139

Peel, M.C., Finlayson, B.L., McMahon, T.A., 2007. Updated world map of the Köppen-Geiger climate classification. Hydrol. Earth Syst. Sci. 11, 1633–1644. https://doi.org/10.5194/hess-11-1633-2007

Rasmussen, R., Liu, C., Ikeda, K., Gochis, D., Yates, D., Chen, F., Tewari, M., Barlage, M., Dudhia, J., Yu, W., Miller, K., Arsenault, K., Grubišić, V., Thompson, G., Gutmann, E., 2011. High-resolution coupled climate runoff simulations of seasonal snowfall over Colorado: A process study of current and warmer climate. J. Clim. 24, 3015–3048. https://doi.org/10.1175/2010JCLI3985.1

Saavedra, F.A., Kampf, S.K., Fassnacht, S.R., Sibold, J.S., 2017. A snow climatology of the Andes Mountains from MODIS snow cover data. Int. J. Climatol. 37, 1526–1539.

Salomonson, V. V., Appel, I., 2004. Estimating fractional snow cover from MODIS using the normalized difference snow index. Remote Sens. Environ. 89, 351–360. https://doi.org/10.1016/j.rse.2003.10.016

Schulz, O., de Jong, C., 2004. Snowmelt and sublimation: field experiments and modelling in the High Atlas Mountains of Morocco. Hydrol. Earth Syst. Sci. 8, 1076–1089. https://doi.org/10.5194/hess-8-1076-2004

Skamarock, W.C., Klemp, J.B., Dudhia, J.B., Gill, D.O., Barker, D.M., Duda, M.G., Huang, X.-Y., Wang, W., Powers, J.G., 2008. A description of the Advanced Research WRF Version 3, NCAR Technical Note TN-475+STR. Tech. Rep. 113. https://doi.org/10.5065/D68S4MVH

Smolarkiewicz, P.K., Margolin, L.G., 1998. MPDATA: A Finite-Difference Solver for Geophysical Flows. J. Comput. Phys. https://doi.org/10.1006/jcph.1998.5901

Sproles, E.A., Nolin, A.W., Rittger, K., Painter, T.H., 2013. Climate change impacts on maritime mountain snowpack in the Oregon Cascades. Hydrol. Earth Syst. Sci. 17, 2581–2597. https://doi.org/10.5194/hess-17-2581-2013

Suzuki, K., Zupanski, M., 2018. Uncertainty in solid precipitation and snow depth prediction for Siberia using the Noah and Noah-MP land surface models. Front. Earth Sci. 12, 672–682. https://doi.org/10.1007/s11707-018-0691-2

Tarek, M., Brissette, F., Arsenault, R., 2019. Evaluation of the ERA5 reanalysis as a potential reference dataset for hydrological modeling over North-America. Hydrol. Earth Syst. Sci. Discuss. 2019, 1–35. https://doi.org/10.5194/hess-2019-316

Telesca, L., Shaban, A., Gascoin, S., Darwich, T., Drapeau, L., Hage, M. El, Faour, G., 2014. Characterization of the time dynamics of monthly satellite snow cover data on Mountain Chains in Lebanon. J. Hydrol. 519, 3214–3222. https://doi.org/10.1016/j.jhydrol.2014.10.037

Thompson, G., Field, P.R., Rasmussen, R.M., Hall, W.D., 2008. Explicit forecasts of winter precipitation using an improved bulk microphysics scheme. Part II: Implementation of a new snow parameterization. Mon. Weather Rev. 136, 5095–5115. https://doi.org/10.1175/2008MWR2387.1

Van Leeuwen, P.J., 2009. Particle filtering in geophysical systems. Mon. Weather Rev. 137, 4089–4114. https://doi.org/10.1175/2009MWR2835.1

van Pelt, W.J.J., Kohler, J., Liston, G.E., Hagen, J.O., Luks, B., Reijmer, C.H., Pohjola, V.A., 2016. Multidecadal climate and seasonal snow conditions in Svalbard. J. Geophys. Res. Earth Surf. 121, 2100–2117. https://doi.org/10.1002/2016JF003999

Verseghy, D.L., 1991. Class—A Canadian land surface scheme for GCMS. I. Soil model. Int. J. Climatol. 11, 111–133. https://doi.org/10.1002/joc.3370110202

Viviroli, D., Dürr, H.H., Messerli, B., Meybeck, M., Weingartner, R., 2007. Mountains of the world, water towers for humanity: Typology, mapping, and global significance. Water Resour. Res. 43. https://doi.org/10.1029/2006WR005653

Von Storch, H., Langenberg, H., Feser, F., 2000. A spectral nudging technique for dynamical downscaling purposes. Mon. Weather Rev. 128, 3664–3673. https://doi.org/10.1175/1520-0493(2000)128<3664:ASNTFD>2.0.CO;2

Waldron, K.M., Paegle, J., Horel, J.D., 1996. Sensitivity of a spectrally filtered and nudged limited-area model to outer model options. Mon. Weather Rev. 124, 529–547. https://doi.org/10.1175/1520-0493(1996)124<0529:SOASFA>2.0.CO;2

Wang, C., Graham, R.M., Wang, K., Gerland, S., Granskog, M.A., 2019. Comparison of ERA5 and ERA-Interim near-surface air temperature, snowfall and precipitation over Arctic sea ice: effects on sea ice thermodynamics and evolution. Cryosphere 13, 1661–1679. https://doi.org/10.5194/tc-13-1661-2019

Wang, D., Morton, D., Masek, J., Wu, A., Nagol, J., Xiong, X., Levy, R., Vermote, E., Wolfe, R., 2012. Impact of sensor degradation on the MODIS NDVI time series. Remote Sens. Environ. 119, 55–61. https://doi.org/10.1016/J.RSE.2011.12.001

Wegmann, M., Orsolini, Y., Dutra, E., Bulygina, O., Sterin, A., Brönnimann, S., 2017. Eurasian snow depth in long-term climate reanalyses. Cryosphere 11, 923–935. https://doi.org/10.5194/tc-11-923-2017

Wu, X., Che, T., Li, X., Wang, N., Yang, X., 2018. Slower Snowmelt in Spring Along With Climate Warming Across the Northern Hemisphere. Geophys. Res. Lett. 45, 12,331-12,339. https://doi.org/10.1029/2018GL079511

Yilmaz, Y., Aalstad, K., Sen, O., 2019. Multiple Remotely Sensed Lines of Evidence for a Depleting Seasonal Snowpack in the Near East. Remote Sens. 11, 483. https://doi.org/10.3390/rs11050483

885

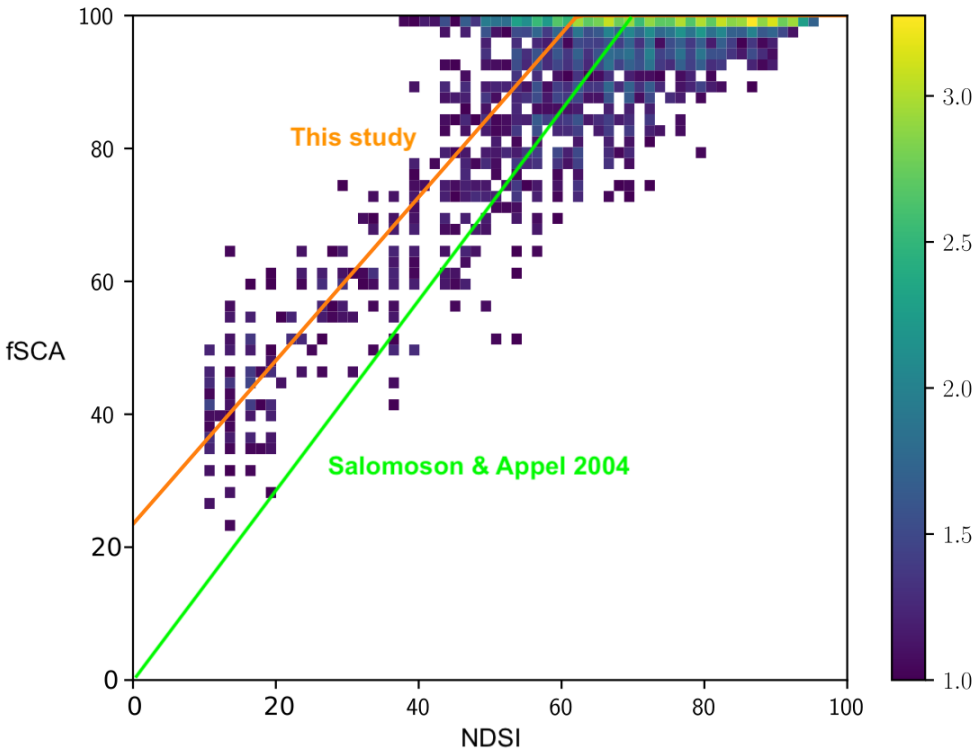

Supplementary 1: Comparison of Salomoson and Appel 2004 function and the newly developed linear equation.